Physicochemical properties of ettringite/meta-ettringite for thermal energy storage: Review

B. Chen, F. Kuznik, M. Horgnies, K. Johannes, V. Morin, E. Gengembre

Physicochemical properties of Ettringite/ Meta-ettringite for thermal energy storage: Review

B. Chen[1, 2,*], F. Kuznik[1], M. Horgnies[2], K. Johannes[1], V. Morin[2], E. Gengembre[2]

[1] Université de Lyon, CNRS, INSA-Lyon, Université Claude Bernard Lyon 1, CETHIL UMR 5008, F-69621, Villeurbanne, France

[2] LafargeHolcim R&D, 95 rue du Montmurier BP15, 38291 Saint Quentin Fallavier, France

* Corresponding author. E-mail address: bao.chen@insa-lyon.fr

Abstract

The cost of materials is one of main obstacles for the development of thermochemical energy storage. Compared with traditional inorganic salt hydrates, a mineral named ettringite can easily overcome this limit thanks to its large resource from cementitious materials. Meanwhile, possession of high energy density (about 500 kWh/m^3), low corrosiveness, non-toxicity and low working temperature (~ 60 °C) around or below common heat resource (solar energy, industrial waste heat, urbane heat system, and even combination with grid) makes ettringite very competitive to be used in an integrated thermal energy storage system. In this paper, the analysis on the available data for structure, preparation of material, thermal conversion, reaction enthalpies, carbonation durability, and ionic substitution of ettringite has been established. Moreover, potential research directions and solutions to improve thermal performance of ettringite-based materials are proposed.

Key Words: Building Materials, Ettringite, Meta-ettringite, Thermal energy storage, Thermochemical energy storage material

Cement notation

A	Alumina (Al_2O_3)
C	Lime (CaO)
H	Water (H_2O)
F	Iron oxide (Fe_2O_3)
S	Silica (SiO_2)
$\bar{S}$	Sulphur trioxide (SO_3)

Abbreviation of phases

AFt	Alumina, ferric oxide, tri-sulfate
AFm	Alumina, ferric oxide, monosulfate
CSA	Calcium sulfoaluminate cement
EttX	Ettringite contains X water molecules per phase
FDDW	Fresh decarbonized demineralized water
MetX	Meta-ettringite contains X water molecules per phase
n	Number of water molecules in per ettringite/ mete-ettringite phase
P_{H2O}	Water vapour pressure (Pa)
P_S	Standard atmosphere pressure (Pa)
RH	Relative humidity (%)
T	Temperature (°C)
TES	Thermal energy storage
w/s	Water-solid weight ratio~~n~~

Contents

1. Introduction

Thermal energy storage (TES), one of the most reasonable solutions to enlarge the application of renewable energy without time and geography limitations, mainly concerns the capture, storage and consumption of thermal energy for later use in different scales (individual house, apartment, district and city). In TES research field, sensible heat and latent heat storage have been widely studied and are presently at an advanced stage of development. On the contrary, thermochemical energy storage techniques are still at initial phase ~~and~~ but provide a relative higher theoretical energy density and a long shelf life without heat dissipation. However, current materials for thermochemical energy storage have a common issue: ~~the~~ high material cost, which limits their wide application and development.

Inorganic pure or composite compounds like $SrBr_2$ hydrates, Zeolite, $MgSO_4$-Zeolithe [1–3] promised to be integrated into thermal energy storage systems with solar collectors. However, material cost, one of main obstacles may hinder the wide use of energy storage systems in real applications. In fact, material selection is always a critical point in the development of energy storage. Several criteria need to be considered [4]:

- ✓ High energy density
- ✓ Low material cost
- ✓ Discharging in usable temperature conditions
- ✓ Regeneration temperature as low as possible
- ✓ Non-corrosiveness
- ✓ Environmentally friendly
- ✓ High specific power (affinity of the sorbent for the sorbate, thermal conductivity, etc.)
- ✓ Moderate operating pressure range
- ✓ Cyclability and stability
- ✓ Sustainability

Being difficult to satisfy all criteria, compromised materials are suggested to be used in thermal energy storage systems. ~~Recent investigations on~~ Ettringite promise~~d~~ potential applications for thermal energy storage since its high energy density (~ 500 kW/h) and large resource from cementitious materials. ~~The~~ Its material cost is as low as 700 \$/m^3 ~~of ettringite~~ [5] in comparison to 4 300 €/m^3 for Silica gel, 2 000 – 3 000 €/m^3 for Zeolite 13-X [6] or more than 42 000 €/m^3 for $SrBr_2$ hydrate [7]. Moreover, non-toxic, no risk of explosion and combustion, and little corrosiveness contrast on most salt ~~energy storage~~ materials make

ettringite a safe material for energy storage. As a cementitious mineral, ettringite has been widely studied for its performances in construction like delayed ettringite formation [8] and expansion phenomena [9,10], but less known, as a thermochemical material. Thus, the review on physical and chemical properties of ettringite seems to be important for its further study in the objective of thermal energy storage.

Ettringite, of which chemical formula is $3CaO{\cdot}Al_2O_3{\cdot}3CaSO_4{\cdot}32H_2O$, or $C_6A\bar{S}_3H_{32}$ as known in cement chemistry notation, is also named as calcium trisulfoaluminate hydrate or AFt in whose group ettringite is one of the most important members. It has a lower density (~ 1.77 $g{\cdot}cm^{-3}$) and contains more water (~ 46%) than any other cement-based hydrates. The modulus and the hardness of ettringite are respectively 20.07 GPa and 0.613 GPa [11]. Ettringite crystals are hexagonal prisms, often elongated with different shapes: needle-like (most general), lath-like or rod-like [12]. After the first report on natural ettringite [13], successful synthesis of high-purity ettringite and its extensive existence in cementitious hydrates announce the possibility for large use. Natural perfect ettringite is transparent but often "coloured" by presence of impurity of metal elements while synthetic ettringite is white powder. However, they share same composition and same crystal phase structure excepting little variation of water content. Most researches ~~on~~ mainly reported ettringite ~~are mainly to study its construction performance in~~ as a building material~~s~~ until a new application as used for thermal energy storage ~~material~~ proposed by Ings and Brown [14]. ~~Considering the link between thermal decomposition behaviour of ettringite and water vapour pressure [14] and further preliminary study~~ Basing on the reported thermal properties in [15,16], ettringite appeared to be a promising material for heat (or cold) storage solutions. Although some advancement has been made in the research of ettringite, such as thermal stability, reversibility [15–17], certain conclusions ~~like on~~ about dehydration process [17–19] and enthalpy [15–17] were not exactly identical.

Same as other salt-based hydrates [1,3,4,20], the principal thermochemical operation on ettringite is based on a reversible process with mass change on water:

$$3CaO{\cdot}Al_2O_3{\cdot}3CaSO_4{\cdot}32H_2O + \text{heat} \leftrightarrow 3CaO{\cdot}Al_2O_3{\cdot}3CaSO_4{\cdot}(32\text{-}X)\,H_2O + X\,H_2O \quad (1)$$

Where X is the number of ~~water~~ removed water per phase ~~during dehydration~~ when dehydrated. During charging cycles, supplied heat from multiple sources, such as solar energy, urban heat system or industry waste heat, makes ettringite dehydrated to meta-ettringite (partially decomposed phase of ettringite) and transferred thermal energy to chemical energy.

For instance, in a single-family house, thermal energy storage using ettringite can be used in summer when solar energy is abundant enough to be collected and transferred as a useful heat resource (**Fig. 1**). Evacuated tube solar air collectors on the roof can provide hot air of high temperature (more than 120 °C) that could easily dehydrate ettringite thanks to the low temperature of dehydration reaction (~ 60 °C) [17]. The higher the temperature of hot air, the better the performance of the system and more heat is stored. Moreover, this material is also compatible with existing hot water solar collectors in individual house as long as a heat exchanger can be installed in the material container. Hot water from solar collector, which temperature could be as high as 100 °C, is therefore supposed to readily withdraw water molecules of ettringite. ~~For example, the hot air/water from domestic solar thermal collector (more than 80°C) could be very appropriate to charge the storage system thanks to the low reaction temperature (~ 60 °C) [17].~~ This good suitability promises a possibility of reducing installation cost of solar system for civil heating use. ~~Contrarily~~ Contrary to dehydration, addition of water (liquid or vapour) on meta-ettringite re-crystallizes ettringite and releases the stored energy (chemical energy → thermal energy). The required water vapour can be from inside or outside humid air and generated humid air, of which relative humidity (RH) should be superior than 60% [17]. ~~This~~ The released heat of hydration depends strongly on the number of removed water per phase referring to X in **Eq. ~~(~~1~~)~~**, typically 1074.1 kJ/mol for 13-hydrate meta-ettringite (Met13, $3CaO{\cdot}Al_2O_3{\cdot}3CaSO_4{\cdot}13H_2O$, X=19) and 1316.1 kJ/mol for Met9 ($3CaO{\cdot}Al_2O_3{\cdot}3CaSO_4{\cdot}9H_2O$, X=23) by hydration with water vapour [17]. Then produced hot dry air is used to heat fresh cold air from outside through a mechanical heat recovery heat exchanger, which delivers heating to the house [1]. Additionally, recent works [17,21–26] have demonstrated the interest of using certain ettringite-based materials to store heat by chemical processes in a building via solar collectors. Therefore, this review is intended to summarize and analyze the physical- and chemical properties of meta-ettringite/ ettringite for thermal energy storage, including phase structure, material preparation, thermal properties (dehydration and ~~re~~hydration), carbonation and phenomena of ion substitution. ~~Potential research directions and solutions to improve thermal performance of ettringite-based cementitious materials are further proposed.~~

2. Formation of ettringite and morphology

Ettringite is a rare mineral phase in nature, while it exists commonly and largely in cement paste. Almost all alumina source, such as $Al(OH)_3$ gel, aluminium sulfate hydrate, C_3A, can

be reactive to form ettringite crystals [18,27,28]: with the addition of some calcium and sulfate source, the desired compound can be obtained under agitation with enough water. Once nucleation of ettringite occurred, the growth of ettringite crystal could be very fast. The crystallization completesd essentially in a few hours with form of lath-like or needle-like [29].

2.1. Conversion based on solutions

The synthesis of ettringite from solutions, which is widely used to prepare pure ettringite, is the most convenient method for a preparation at the lab scale. The main process of conversion could be expressed by the following reaction:

$$Al_2(SO_4)_3{\cdot}XH_2O + 6\ Ca(OH)_2 + (26\text{-}X)\ H_2O \rightarrow 3CaO{\cdot}Al_2O_3{\cdot}3CaSO_4{\cdot}32H_2O \quad (2)$$

Where X= 14-18.

As mentioned in **Eq. (2)**, $Ca(OH)_2$ and $Al_2(SO_4)_3{\cdot}XH_2O$ are used as CaO and Al_2O_3–SO_3 source respectively. In order to get pure ettringite, analytical grade reagents are recommended. The first step is to make a saturated $Ca(OH)_2$ solution by having an appropriate amount of fresh sintered CaO dissolved in some fresh decarbonized demineralized water (FDDW). After the stoichiometric addition of diluted $Al_2(SO_4)_3 \cdot XH_2O$ solution (with FDDW) into the former $Ca(OH)_2$ solution which is cooled down in a fridge, the suspension is needs to be well stirred for 3 hours. Once the produced compound is filtered in vacuum and washed by FDDW and ethanol, the powder sample is finally dried and stored in a desiccator (containing $CaCl_2$ saturated solution who gives about 35% relative humidity [30]). All the above operations are under protection of N_2. Some investigators [15,31] suggested that the initial introduction of sugar in $Ca(OH)_2$ solution was preferable to increase its solubility of about 0.02 to 0.3 mol/L. This solution conversion method was similarly described in other reports [19,30,32,33] and only a trace of monosulfate or calcium carbonate has been detected in several separated studies [34–36].

2.2. Conversion based on solids

Different from solution conversion method, solid reactive oxides are main precursor to synthesize ettringite. The preparation of these components could be long because of repeatedly on-going grinding and calcination until fine powder. Moreover, a curing for of several days for the hydration of cement compositions is necessary.

2.2.1. *Ettringite conversed by CA or C_3A*

CA and C_3A, which are prepared from the calcination of a stoichiometric mixture between Al_2O_3 and CaO (or $CaCO_3$), belong to active aluminates with different contents of calcium. Ettringite crystallizes in an aluminate-rich gel, which is a mixture of appropriate amount of CaO (not for C_3A) and $CaSO_4 \cdot 2H_2O$ with sufficient FDDW. This process is strongly exothermic. After ~~a~~ curing ~~of several days~~, ettringite samples can be vacuum-filtered under protection of N_2. Main chemical reactions could be [37]:

$$CaO \cdot Al_2O_3 + 2\ CaO + 3\ CaSO_4 \cdot 2H_2O + 30\ H_2O \rightarrow 3CaO \cdot Al_2O_3 \cdot 3CaSO_4 \cdot 32H_2O \quad (2)$$

$$3CaO \cdot Al_2O_3 + 3\ CaSO_4 \cdot 2H_2O + 30\ H_2O \rightarrow 3CaO \cdot Al_2O_3 \cdot 3CaSO_4 \cdot 32H_2O \quad (3)$$

2.2.2. *Ettringite conversed by $C_4A_3\bar{S}$*

There are two different methods: direct and indirect to produce $C_4A_3\bar{S}$ [38]. It is possible to synthesize directly $C_4A_3\bar{S}$ from a stoichiometric mixture of $CaCO_3$, $CaSO_4 \cdot 2H_2O$ and Al_2O_3 at about 1200 °C while the second way is to sinter a mixture of C_3A ~~mentioned before~~, gypsum and $Ca(OH)_2$. These two methods have been proved successful to yield high purity $C_4A_3\bar{S}$. An intimate stoichiometric mixture of $C_4A_3\bar{S}$, $CaSO_4$ and $Ca(OH)_2$ ~~was~~ is then prepared and hydrated with a water to solid (w/s) ratio of 0.6 using FDDW. After ~~a~~ curing at certain conditions, very pure ettringite can be obtained. The hydration process is as following:

$$4CaO \cdot 3Al_2O_3 \cdot SO_3 + 5\ CaSO_4 + 9\ Ca(OH)_2 + 87\ H_2O \rightarrow 3\ (3CaO \cdot Al_2O_3 \cdot 3CaSO_4 \cdot 32H_2O) \quad (4)$$

Although these solid conversion processes are slow, they result a product getting rid of other potential chemical impurities. Grusczscinski et al. [39] used commercial pure Calcium aluminate sulfate ($C_4A_3\bar{S}$) phase and self-prepared C_3A respectively to synthesize ettringite powder. Zhou et al. [40] prepared a mixture of 0.02 moles of C_3A and 0.06 moles of $CaSO_4 \cdot 2H_2O$ to react with excessive degassed, deionized water (w/s=11). After 10 days of agitation in a closed vessel, ettringite crystals of about 10-20 μm with traces of amorphous material were harvested. Similar preparation process was also reported with a higher w/s ratio of 20 [17]. Other compounds like $C_6A\bar{S}$ [41] and $C_{12}A_7$ [42] were equally described to obtain pure ettringite.

2.2.3. *"Alumina, ferric oxide, monosulfate (AFm)" transformation method*

AFm, chemical formula of $3CaO \cdot Al_2O_3 \cdot CaSO_4 \cdot nH_2O$ (n=12–14), as a hydrate of Portland cement paste, is compound of C_3A, $CaSO_4$ (anhydrite) and water, only in different

proportions compared with ettringite. Between these binomials, a mutual transformation can occur with presence of C_3A (form AFm) while with excessive $CaSO_4$ to form Aft phase:

$$2\ (3CaO{\cdot}Al_2O_3) + 4\ H_2O + 3CaO{\cdot}Al_2O_3{\cdot}3CaSO_4{\cdot}32H_2O \rightarrow 3\ (3CaO{\cdot}Al_2O_3{\cdot}CaSO_4{\cdot}12H_2O) \quad (5)$$

$$3CaO{\cdot}Al_2O_3{\cdot}CaSO_4{\cdot}12H_2O + 2\ CaSO_4\ (\text{excessive}) + 20\ H_2O \rightarrow 3CaO{\cdot}Al_2O_3{\cdot}3CaSO_4{\cdot}32H_2O \quad (6)$$

With respect to this principle, Pan et al. [43] mixed self-prepared CA of high purity with CaO and $CaSO_4{\cdot}1/2H_2O$ by a ratio of w/s=4. After a ~~sealing~~ sealed curing of 7 days, pure AFm was available. Afterwards, AFt could be conversed via a deep hydration of AFm with water and excessive gypsum.

2.3. Mechanism of formation

Peng and Lou [44] described the relation between evolution of ion concentration and formation of ettringite by solid phase analysis and ion concentration analysis in aqueous phase. They thought the three above chemical processes had a same chemical mechanism: the minerals dissolved rapidly to produce Ca^{2+}, SO_4^{2-} , OH^-, and then a saturated solution of ettringite was prepared. These ions moved together under the effect of ion concentration gradient (after nucleation of ettringite). Thus, ettringite crystals could be formed according to three following steps:

$$AlO_2^- + 2\ OH^- + 2\ H_2O \rightarrow [Al(OH)_6]^{3-} \quad (7)$$

$$2\ [Al(OH)_6]^{3-} + 6\ Ca^{2+} + 24\ H_2O \rightarrow \{Ca_6[Al(OH)_6]{\cdot}24H_2O\}^{6+} \quad (8)$$

$$\{Ca_6[Al(OH)_6]{\cdot}24H_2O\}^{6+} + 3\ SO_4^{2-} + 2\ H_2O \rightarrow \{Ca_6[Al(OH)_6]{\cdot}24H_2O\}(SO_4)_3{\cdot}2H_2O \quad (9)$$

Brown and LaCroix [45] concluded that the formation rate of ettringite based on C_3A was controlled by a diffusional process with apparent activation energy of formation of 1 kcal/mol and probably a one-dimension growth to form a needle-like morphology. A liquid interlayer (zone of diffusion) was reported between the solid phase ($C_4A_3\bar{S}$) and the formed crystal of ettringite (**Fig. 2**) [46]. In this interlayer, whose thickness was depended on the concentration of ions, a saturated solution of ettringite was created (**Eq. 7 and 8**). Ettringite then crystallized in the solution of high pH>10.7 (**Eq. 9**). Grusczscinski et al. [39] confirmed this interspace by SEM and ex situ formation mechanism by the appearance of independent ettringite crystal from C_3A.

3. Crystal structure

3.1. Structure of ettringite crystals

Aluminium and calcium show respectively chemical valences of +3 and +2 when consist of binaries between Al-O and Ca-O. Based on this knowledge, Bannister et al. [47] on the first time proposed that the crystal structure is constructed on hexagonal (**a**=11.24 ± 0.02 Å, **c**=21.45 ± 0.05 Å, space group of D_{4h}^{6} ($P6_3/mmc$) and Z=2) with a content of $12CaO{\cdot}2Al_2O_3{\cdot}6SO_3{\cdot}64H_2O$ via X-Ray patterns for natural ettringite. Some "zeolitic" water molecules were predicted to locate in the channels which are parallel to the c-axis (0001) while aluminium atoms were hypothetically barred in $Al(OH)_6^{3-}$ octahedral groups. Other investigations on the structure of different ettringite crystals confirmed the lattice parameters with little variation due to the source of specimen (Table 1). Meanwhile the specific gravities of ettringite ranged generally between 1.75 and 1.78 via the calculation by **Eq. (10)**:

$$D = ZM/N_AV \quad (10)$$

Where D is the density, Z-factor = 2, M is the molar mass of hydrate, V is the volume of unit cell calculated based on the lattice parameters from X-ray Diffraction (XRD) and N_A is the Avogardro's number.

Table 1. Comparison for lattice parameters of ettringite from different localities

Locality	a (Å)	c (Å)	Specific Gravity	References
Crestmore	22.33* / 2 =11.165	21.35*	1.78	[48]
Ettringiten	22.48 / 2 =11.24	21.31	1.762**	[48]
Scawt Hill	11.24	21.45	1.772	[47]
	11.23	10.75 × 2 = 21.50	1.750**	[49,50]
Kalahari Manganese Field	11.223 [a]	21.474 [a]	1.754 [a]	[27]
	11.229 [b]	10.732 [b] × 2 =21.464	1.753 [b]	[27]
N'Chwanning mine	11.240	21.468	1.749**	[51]
	11.2530	21.6436	1.731**	[36]
Synthetic samples	11.167	21.360	1.9	[52]
	11.23	21.49	1.750**	[19]
	11.167	21.354	1.781**	[53]
	11.229	21.478	1.772**	[54]
	11.211–11.225 [c]	21.451– 21.478 [c]	1.753-1.759**	[31]

	11.2220 [d]	21.4327 [d]	1.758**	[30]
	11.2129 [f]	21.4783 [f]	1.757**	[30]
	11.2514	22.6788	1.652**	[36]

* Ettringite from Crestmore contained a detectable amount of CO_2 [48], which therefore probably modified the lattice parameters.

** The parameters were doubled and the ~~special~~ specific gravities were calculated with an assigned composition $Al_2O_3 \cdot 6CaO \cdot 3SO_3 \cdot 31H_2O$.

a: Supercell, special gravity calculated with an assigned composition $Al_2O_3 \cdot 6CaO \cdot 3SO_3 \cdot 31H_2O$.

b: Subcell, special gravity calculated with an assigned composition $Al_2O_3 \cdot 6CaO \cdot 3SO_3 \cdot 31H_2O$.

c: The values varied with the ratio of Ca/Al.

d: Dry ettringite (dried at 35% relative humidity over saturated $CaCl_2$ solution).

f: Wet ettringite stored in the mother liquid of synthesis.

McConnell and Murdoch [55] pointed out the similarities in physical parameters between thaumasite and ettringite, and predicted that the structures of these crystals must be closely related. Yet Bezjak and Jelenic [56] thought the layers of Al-O and Ca-O polyhedral were perpendicular to c-axis with little support from other investigations. Moore and Taylor [49] verified the space group of ettringite (*P*31c) and further proposed a detailed crystal structure: ettringite consists of column structure ($[Ca_6[Al(OH)_6]_2 \cdot 24H_2O]^{6+}$, per half of unit cell) running parallel to **c** and channel components (SO_4^{2-} and H_2O). The core of column structure is the aluminium oxide octahedron $[Al(OH)_6]^{3-}$ which is linked to three adjacent calcium atoms by bonds of Al-OH-Ca. The 8-coordinated Ca^{2+} ions are located in a polyhedral (probably a trigonal prism with two additional vertices) composed by four hydroxyls and four H_2O molecules (as shown in **Fig. 3**). This basic structure of ettringite (a nearly cylindrical shape) is oppositely twice the structure of columnar core along the longitudinal axis with a repeatable distance of 10.75 Å (about half of **c**-parameter) and a space group *P*31c. In the channels, three SO_4^{2-} ions and two water molecules ($[(SO_4)_3 \cdot 2H_2O]^{6-}$, per half of unit cell) occur in four positions, of which only one for 2 H_2O group (0.25 possibilities). These components are supposed to be, at least, partially ordered. With the hypothesis of zero twist between the sulfate tetrahedral and water groups, the arrangement for *P*31c is then inferred as $P6_3$ for ettringite crystals [50]. Moreover, the hydrogen bonds are considered as the liaisons between column structures and channel materials. The positive charge of column structure from Ca^{2+} and Al^{3+} ions is distributed among the H_2O molecule combine with Ca atoms, which means that the whole surface of column is positively charged [50]. Therefore, every

sulfate tetrahedral (negatively charged) interact with all the around columns to keep totally electrically neutral.

Berliner et al. [52] confirmed the basic column structure (*P*31c space group with **a** = 1.11670(5) nm and **c** = 2.13603(13) nm) and channel components proposed by Moore and Taylor [50] via the investigation of a synthetic ettringite by neutron powder diffraction techniques with a reactor-based instrument. Hartman and Berliner [53] synthesized an ettringite having deuterium in place of hydrogen and confirmed again the column structure of a synthetic ettringite was in the *P*31c space group (**a**≈11.16 Å, **c**≈21.35 Å) excepting that oxygen atoms were slightly shifted compared with [50]. The overall column structure based on Al- and Ca-polyhedral remained still unchanged. Renaudin et al. [30] indicated a small difference of lattice parameters between wet and dry ettringite. The crystal of ettringite was showed to become slightly shorter (~0.0182 Å) and wider (~0.0456 Å) after drying treatment.

In addition, different interatomic distances in the column structure have been also reported in **Table 2**. Skoblinskaya and Krasilnikov [57] have summarized a similar table for unit cell of ettringite from the detailed work by Moore and Taylor [50]. However, their synthesis of data would be probably more reasonable with the consideration that the interatomic distances may change more or less during the removal of combined water in the column. Goetz-Neunhoeffer and Neubauer [54] also described a revised ettringite structural model with the considering of 128 positions for H at room temperature. In their ~~model~~ proposition, there existed a shift for every atom (Al atoms as reference at original point), which had also a certain difference from the values reported in [50,53]; meanwhile the lengths of chemical bonds were increased or decreased accordingly.

Table 2. Information about some important interatomic bond (related to Fig. 3)

Type of bond	[50]		[54]		Comments (correspond to **Fig. 3**)
	Distance (Å)	Bond angles (°)	Distance (Å)	Bond angles (°)	
O-Al-O	1.82 – 2.00	84.7 – 95.6	1.82 –1.88	79.3 – 96.2	/
O-Ca-O	2.60 – 2.75	64.7 – 93.0 (angles above 115° not given)	2.25 – 2.83	/	Ca(1) – O(10,12) Ca(2) – O(9, 11)
	2.36 – 2.56		2.35 – 2.63		Ca(1) – O(6,8) Ca(2) – O(5, 7)
	2.35 – 2.52		2.36 – 2.48		Ca(1) – O(1, 3) Ca(2) – O(2, 4)
S-O	1.31 – 1.56	105.6 – 113.2	1.44 – 1.51	105.8 – 112.9	/

Hartman and Berliner [53] exhaustively studied the hydrogen bond network in ettringite using the ettringite structural refinement model investigated by high-solution time-of-flight neutron powder diffraction techniques. The length of relevant bonds and corresponding angles were summarized in **Table 3**. In the unit cell configuration of ettringite (**Fig. 4**), hydrogen bonds ranging from 1.708 to 2.347 Å denoted a longer distance than normal O-H chemical bond (typically 0.962 Å). From the illustration, it was clearly seen that the hydrogen bond network acted very importantly to stabilize the crystal structure of ettringite and meanwhile played a connective role between neighbour column structures. Renaudin et al. [30] reported the environment of sulfate ions and water groups by Raman spectroscopy. In their model, each sulfate ion was adhered in the inter-column space by twelve hydrogen bonds to twelve water molecules bonded to calcium atoms and four hydrogen bonds to four water molecules coordinated to Ca for each channel water molecule~~s~~.

Table 3. Summary of hydrogen bonds in deuterated ettringite [53]

Group	Type of bond	Distance (Å)	Bond angles (°)
Hydroxyls	O-D–O	2.130–2.347	151.0–173.0
Water molecules		1.708–2.223	110.6–173.1

Note: O-D presents chemical bond and hydrogen bond is given as D–O.

In brief, most investigations agree that the **a**-parameter and **c**-parameter of ettringite locate respectively at 11.165~11,253 Å and 21.310~21,679 Å with a specific gravity of 1.750~1.781. The crystal structure of ettringite is stabilized not only by the chemical bonds like Al-O and Ca-O in the column, but also by the network of hydrogen bonds for inter-column distance and adhesion of channel compositions.

3.2. Structure of meta-ettringite

Seen water molecules linked to cations by chemical covalent bonds, the dehydration process to remove these molecules will create vacancies of electrons, which trends to arrange the remaining chemical ~~bounds~~ bonds and produce a new structure formation.

During the water removal process of ettringite, the horizontal thermal expansion was reported as twice as the one parallel to **c**-axis in range 70 – 110 °C [58]. With a removal of 34.4% weight after dehydration at 110 °C, the mean refractive index rose from 1.46 (negative) to 1.50 (positive) for Met8[1]. After the arrangement of structure, the dehydrated single crystal

[1] Calculated basing on an initial formula of $3CaO{\cdot}Al_2O_3{\cdot}3CaSO_4{\cdot}32H_2O$.

was described as an oriented pseudo-morph with approximate cell sides **a** = 8.4 Å, **c** = 10.21 Å accompanying a lattice shrinkage mainly in the plane perpendicular to **c** axis. The rest compound got a space-group of ***C***6/mmc [47]. Skoblinskaya et al. [59] verified the trends of growth of average refractive index during the dehydration process. A meta-ettringite of 18-hydrate with a decreased of inter-column distance (9.73 Å) could still keep a negative elongation, which means that the crystal structure of ettringite has been retained. Moreover, the interplanar distance of a further dehydrated meta-ettringite of 12-hydrate arrived 5.2~5.7 Å (referring to a wide diffuse in X-ray o'grams). Inconsistently, Shimada and Young [32] reported a slight decrease of **c**-parameter (from 21.46 to 21.04 Å after a loss of 15 water molecules) unlike the reported halved value [47] and contrary trend for **a**-parameter, which increased from 11.22 to 11.52 Å. Similar results were also demonstrated for amorphous Met12 by inferring directly occupancies from diffraction data [60]. Differently, another investigation [40] showed that the **c**-parameter down to half after being dehydrated to a 11~13-hydrate (calculated volume = 663.3 $Å^3$ given by [17]) while **a**-parameter markedly decreased from 11.23 to 8.49 Å by Selected Area Electron Diffraction (SAED) patterns, very close to the values reported in [47]. Apart from thermal process, ettringite has also been reported owing a reversible transformation to an amorphous phase under 3 GPa with the reduction of both **a**- and **c**-parameter [51]. What's more, the specific surface area by Brunauer-Emmett-Teller (BET) theory increased at least 7.8% after the dehydration of ettringite to a 13-hydrate [40], which was indicated to keep long-range order under an in-situ observation [60]. Mantellato et al. [33] demonstrated that AFt phase was possible to lose 12 water molecules at moderate temperature and 0% RH, which did not modify its specific surface area (SSA). The coordination number of Ca and Al was reported respectively to reduce from 6 to 4 after a total dehydration (Met0) [32,57,59]. Baquerizo et al. [17] proposed a negative correlation between density and water content for ettringite and meta-ettringite:

$$\text{Density} = 2600 - 29.25n \qquad (11)$$

Where n presents the number of water molecule in unit structure.

The above section suggests, more or less, the change of the lattice parameter of ettringite after dehydration. The reported variations of lattice parameters were indeed not identical. Whereas, the reduction tendency of **c**-parameter seems to be same point in different investigations, while for **a**-parameter is still not clear (increase or decrease). Overall, the

removal of chemically combined water molecules in column structures could essentially make the crystallinity reduced until to be amorphous companying an increase of density.

4. Thermal properties of ettringite and meta-ettringite

The phenomenon of mutual transformation accompanied by water mass change for the binomial, ettringite and meta-ettringite, have been already successfully confirmed for the storage of thermal energy by previous works [15,17,61]. Thanks to its high content of water, the ideal energy storage density could be higher than 500 kWh/m^3 (for Ett32 ↔ Met 9 [17]). However, the released heat strongly depends on the quantity and status of absorbed water. Theoretically, water vapour gives a higher value than liquid water with a difference of 40.65 kJ/mol H_2O at 25 °C (enthalpy of condensation of water vapour).

4.1. Decomposition and dehydration

The decomposition of ettringite here mainly relates to the reaction with water to reform a new crystal, which can reform ettringite under certain conditions. Dehydration, often referring to thermal dehydration, is also named as process of storing energy, which means only the partial or total removal of water molecules in ettringite crystal. The thermal characterization of the dehydration process mainly describe thermodynamic analysis, using Thermogravimetric Analysis (TGA) and Differential Scanning Calorimetry (DSC) with different heating rates and temperatures, often accompanied XRD analysis, Fourier-transform infrared spectroscopy (FTIR) or Raman spectroscopy analysis. As a thermodynamic and kinetic process, the dehydration of ettringite is not only temperature-dependent also humidity- and time-dependent.

4.1.1. Decomposition

Ettringite has been reported existing in its aqueous solution up to 90 °C [62] giving the little solubility of ettringite in water [19,63]. Similarly under saturated steam (100% RH), ettringite was more resistant than under dry condition: no obvious change at 93 °C. However, at 149 °C, ettringite decomposed to monosulfate [64], which was calculated to be more stable than trisulfate hydrate (ettringite) during its formation above 70 °C [65]. A hydrogarnet phase ($3CaO{\cdot}Al_2O_3{\cdot}6H_2O$, C_3AH_6) was further detected at 232 °C in autoclave. This process of hygrothermal decomposition hasd been detailed by three endothermic steps, as following [42]:

399 $C_6A\bar{S}H_{32}(s)$[2] → $C_4A\bar{S}H_{12}(s)$ (monosulfate) + 2 $C\bar{S}H_{0.5}$ +19H (l) 111 < T < 190 °C (12)

400 $C_4A\bar{S}H_{12}(s) \rightarrow C_3AH_6(s) + C\bar{S}$ (s) +6H (l) 190 < T < 280 °C (13)

401 3 $C_3AH_6(s) \rightarrow C_4A_3H_3(s)$ +5CH(s) + 10H (l) T > 280 °C (14)

402 Some other investigations [38,58] also supported that ettringite decomposed to monosulfate in
403 the range 114 – 150 °C with a high pressure while in contact with aqueous phase. Somehow,
404 the thermal stability of ettringite was enhanced in a solution. From other side, ettringite was
405 confirmed to be definitely stable by a heat treatment at 80 °C in distilled water for 12 hours
406 [35] and even at 107 °C with a pressure of 150 kPa [66]. Thorough the calculation of the
407 stable zone for ettringite in the $CaO\text{-}Al_2O_3\text{-}SO_3\text{-}H_2O$ system at 25, 50 and 85 °C respectively,
408 Damidot and Glasser [67,68] indicated that ettringite was chemically less stable at a higher
409 temperature. Kaufmann and his co-workers [69] indicated that ettringite in a CSA cement
410 block was calculated stable up to 90 °C under steam treatment and it decomposed
411 experimentally to monosulfate (AFm) under steam curing condition at temperatures far below
412 100 °C for a CSA cement system. The AFm phase was considered unstable and decomposed
413 to katoite[3] if at a higher temperature (> 100 °C).

414 ***4.1.2. Dehydration***

415 Without contact with an aqueous phase, ettringite was supposed to dehydrate itself into
416 meta-ettringite when heated. This process of Ett30 to Met12 manifested that the Arrhenius
417 law only gave a good approximation at 55 – 70 °C with the growth of meta-ettringite from the
418 surface to internal controlled by a rate-limiting step at the interface between ettringite and
419 meta-ettringite [70]. However, the reported dehydration temperature and process from
420 different researches were not identical. Ings and Brown [14] found three endothermic peaks
421 for this process by using DSC; only the third peak at about 100 °C showed a large quantity of
422 heat (426.8 J/g) compared with 33.5 J/g at 33 °C and 405.8 J/g at 90 °C. Moreover, the
423 endothermic process started at very beginning (about 30 °C) according to the DSC curve. This
424 "advanced" dehydration at low temperature was also demonstrated in other studies [15,16,19].
425 As for in Thermogravimetry (TG), the removal of 30.7 water molecules were detected for a
426 synthetic ettringite: 21– 22 water molecules lost up to 70 °C and another 9-10 H_2O were lost
427 between 70 and 1000 °C [18]. Perkins and Palmer [19] assigned that the dehydration in TGA
428 were separated to three steps: first loss of about 23 water molecules (33% of mass loss)

[2] Maybe for the reason of typographical error, the formula should be written as $C_6A\bar{S}_3H_{32}$.
[3] $Ca_3Al_2(SiO_4)_{3-x}(OH)_{4x}$ x=1.5-3

between 40 and 180 °C, then 3 molecules in range 200 – 280 °C and others 3 between 280 and 500 °C. Similar process was also reported by Jiménez and Prieto [36] for natural and synthetic ettringite accompanied with some difference on the mass loss of water may due to their different initial water content and the perfection degree of crystals. Natural ettringite was still indicative in XRD after a heat treatment at 260 °C for 7h by TG [27], which also declared the different behaviours between synthetic and natural ettringite. Furthermore, Abo-El-Enein et al. [71] concluded that the morphology of ettringite affected the dehydration process, which may explain why the weight loss obtained from thermal analysis was often smaller than the loss calculated based on chemical composition. Besides the main dehydration peak at 110 °C, Ogawa and Roy [38,72] divided the location of peaks at less than 350 °C by DSC with a low heating rate (1 °C/min): one at 160 °C and the other at 250 °C. As no obvious change of X-ray patterns for the samples heated at temperatures both above, these peaks corresponded exactly to the further removal of water after 110 °C.

Moreover, a large sample of ettringite (at level of gram) seemed much more resistant in an oven than a small one (in order of milligram) in the TGA or DSC. Ettringite was indicated stable below 66 °C and decomposed partially at 93 °C in a drying oven [64]. According to Struble and Brown [15], a sample of several grams of Ettringite dehydrated in an oven at 56 °C with only 14% mass loss after 72 h while 27% loss of a sample of 1 mg at 51 °C in 40 minutes by TGA. This resistance was overcome by a doubled temperature for 2 h in the oven. Else, a couple of days and 0% RH were necessary to remove about 21 water molecules per phase at 40 °C or much longer at 25 °C [16]. Abo-el-Enein et al. [71] determined the mass loss of ettringite at different temperature under 100 °C, and especially an approximate removal of 20 water molecules per phase at 58 °C [73]. Shimada and Young [32] demonstrated the effect of temperature on the same ettringite samples (at level of gram): a 3-water-molecules loss at 60 °C, then progressive loss of 20 – 21 H_2O at 70 – 80 °C and 24 – 25 at 100 – 120 °C. Zhou and Glasser [61] showed that the temperature of dehydration was directly related to environment humidity. ~~The bigger humidity in the system was, the higher temperature for dehydration needed.~~ Baquerizo et al. [17] also indicated that a higher temperature was required in a high humidity system than in dry environment. According to [23], ettringite in CSA paste could lose totally its crystallinity at 60 °C and low vapour pressure (3% – 8% RH) for 3 days, which verified the disappearance of ettringite peaks in XRD for some CSA blocks after drying at 90 °C [69].

The natures of matter are always related to structure, so does ettringite. Considering its structure, the removal of water from ettringite may be separated roughly into two ~~steps~~ parts: zeolitic water in the channels and covalently combined water in the columns.

i. Zeolitic water of ettringite in the channels

For a single phase, ettringite theoretically contains 32 molecules of water, 30 of which are regularized in the columns networks and only 2 are linked loosely in the channels as "zeolitic water". A few reports stated an ettringite containing 36 molecules of water, from which 6 were zeolitic water molecules [74], but easily to lose and decrease to 30 when dried at 25 °C. This loss of channel water controlled by relative humidity (RH) at around 18 °C would not change properties even down to 0.05 P_S (standard pressure) [57]. Renaudin et al. [30] confirmed that no structural modification occurred after losing these zeolitic waters except a slight increase on **a**-parameter and a decrease of **c**-parameter.

ii. Column water of ettringite

The remained water ($n \leqslant 30$) is known as structural composition for the network of ettringite. If n goes below 30, the crystal undergoes structural modification. This process was then detailed by Skoblinskaya et al. [59] by 3 divided steps for removal of water.

The first loss of 12 H_2O ~~bounded~~ linked to Ca atom ($n= 30 \rightarrow n= 18$) was said to not change the crystal structure since the residual 18 H_2O hydrate kept a same negative elongation and refractive index. Moreover, the typical peaks of ettringite were still very recognizable in X-ray diffraction patterns. However, **a**-parameter decreased approximately from 11.23 Å to 9.73 Å considering that the broadening of diffraction lines could lead to an inaccurate determination.

The next loss of 12 H_2O also from Ca atom ($n= 18 \rightarrow n= 6$) required harsher experimental conditions. Firstly, very low pressure (20 Pa) was necessary to withdraw 6 H_2O located at main apex of Ca-polyhedral. This process distorted the ettringite structure, the columns were relatively arranged and the decomposition product was said to be amorphous, of which **a**-parameter was about 8.5 Å [40]. Differently, Bannister et al. [47] indicated that the odd layer-lines of a rotation photograph of ettringite dehydrated at 110 °C along the c-axis were weak, which corresponded to a sideways shrinkage of lattice but very little change along the c-axis. The increase of **a**-parameter and the contrary change of **c**-parameter during the dehydration of ettringite at 70 °C were also described by Shimada and Young [32]. Then, a high temperature

(180 °C) made n down to 6. Meanwhile, a second reduction of **a**-parameter was considered to cause the collapse of channels and brought the columns closer. As a result, new chemical bonds might be arranged between SO_4^{2-} and columns. The halved **c**-parameter [47] was probably caused by the strengthening of remained Ca-O bonds after the re-distribution of electrons of Ca.

The withdrawal of last 6 water molecules started at 180 °C or higher and 0.8 Pa. Chemical bonds could be surely reorganized because of the absence of OH groups between Al and Ca atoms. However, these new bonds were said to exist neither in all ettringite crystals nor in the whole volume of crystalline. If the dehydration went rapidly (about 120s), fewer bonds were constructed while ruptures inside the crystals and voids formed with increasing expansion of crystals [59]. Briefly, the process of dehydration of ettringite can be summarized as following in **Table 4**:

Table 4. Structure and water number per unit cell of ettringite during withdrawal process [32,50,57,59]

Step number	Position and form of bond of water molecules		Interatomic distance (Å)		The number of water molecules of a given form of bond	The number of remaining water	Coordination number of Ca (Al)	Condition to withdraw corresponding water molecules
1	Water in channels	/	Ca-O	5.06 and 7.47	1.7	30	8 (6)	Temperature: 18 °C Pressure: ~0.05 P_s
2	Water in columns	In the additional vertices of the trigonal prisms	Ca-O	2.60 – 2.75	12	18	8 (6)	First 6 molecules: Temperature: 18 °C Pressure: ~20 Pa
3		In the main vertices of trigonal prisms	Ca-O	2.36 – 2.56	12	6	5 (6)	Temperature: 18 – 180 °C Pressure: ~20 Pa> P> ~0.8 Pa
4		In a hydroxyl form in the Al and Ca polyhedral of columns	Al-O	1.82 – 2.00	6	0	4 (4)	Temperature: >180 °C Pressure: ~0.8 Pa
			Ca-O	2.35 – 2.52				

However, this gradual dehydration process related to the structure of ettringite has not been ~~encountered~~ confirmed by dynamic characterization methods, such as differential thermal analysis (DTA) [61], TG and DSC [14–17,36]. ~~Even having studied the previous~~

~~numerous TG and DSC analysis, this process was still not clearly determined.~~ Being contrast to a stepwise dehydration, the work of [60] demonstrated that the remove of water molecules linked to different atoms occurred simultaneously at 50 °C. Briefly, the existence of stepwise dehydration process still needs to be verified by experimental methods.

4.2. Hydration

Hydration of meta-ettringite, the reversible process of dehydration, refers to the regain of moved water molecules and reforms hydrates of a higher degree than that of the dehydrated material, and often reproduces ettringite crystals from amorphous phases. This process is usually characterized by Sorption Calorimetry, Dynamic Vapour Sorption (DVS), DSC, TGA and XRD. Same as dehydration of ettringite, the hydration of meta-ettringite is also temperature-, humidity- and time-dependent. Moreover, the hydration process ~~was~~ has been indicated ~~very rapid,~~ releasing the majority of heat within 10 seconds while in contact with liquid water [14].

Bannister et al. [47] reported that the dehydration process was reversible if the residual material (after a treatment at 110 °C) was left in moist air for a sufficiently long period. This phenomenon has even been confirmed for the product after TG analysis up to 1000 °C [16], which is supposed to be similar with the hydration of cement material. Giving by [58], the dehydration process of ettringite was reversible at a low temperature for ettringite. Kira et al. [75] also concluded that the short-range order structure of ettringite heated up to 500 °C could recrystallize by the hydration above 60% RH at 20 °C. Zhou and Glasser [61] completed ~~that~~ the hydration at different determined temperature (< 120 °C) with an error of ± 2.5-5 °C. Moreover, a low temperature and a high humidity environment seemed to favor the crystallization of ettringite and ~~to~~ reduce the time of formation. The maximum water molecule number of hydrated ettringite in per phase (n_{max}), which negatively correlated to the dehydration degree, could increase up to 36.5 [57] containing about 6 “zeolitic water” molecules [74]. In fact, the excessive water molecules might be adsorbed in crystal defects or just on the crystal surfaces, for which the quantification and localization were difficult. This dehydration/ hydration cycle was repeatable for massive ettringite samples (1 – 2 g), and after several cycles, ettringite was still able to be reformed in moist nitrogen gas from dehydrated products at 40 °C and 0% RH [16]. Some gypsum was detectable by X-ray patterns during the hydration experiments [61]. All these hydration processes probably started with some condensation in the defects or on the surface. Hence, a local through-solution nucleation mechanism leaded to reformation of ettringite [61]. Baquerizo et al. [17] executed the

hydration of Met 9 to determine the relation between hydrate state and enthalpy of mixing by isothermal sorption and sorption calorimetry at 25 °C. Furthermore, the results seemed to suggest a possible gradual hydration process: A peak of exothermic enthalpy (17 kJ/mol H_2O) appeared while n was supposed to be between 12 and 14 showing a probably relative change of structure. Continually, the hydration process could be considered as stable between n= 14 and 30 since the enthalpy stabilized at about 13.3 kJ/mol H_2O while the sorption of two "zeolitic water" molecules only released 6.0 kJ/mol H_2O.

Some investigators [23,69] also reported this reversibility of ettringite in CSA cement paste along with a harmful effect on the mechanic performance of sample. This damage may be caused by the change of ettringite morphology relating to the variation of **a**- and **c**-parameters and a possible change of crystal structure [40] during the cycle process of dehydration and rehydration.

4.3. Dehydration and hydration modelling of ettringite vs. meta-ettringite

As mentioned above, the dehydration and hydration processes are related inseparably to humidity and temperature. In addition, the reversible phenomenon between ettringite and meta-ettringite has been already reported to be repeatable under different humidity conditions [16].

The detailed work by Zhou and Glasser [61] firstly demonstrated the thermal stability of ettringite under a controlled environment (temperature and water vapour pressure), with a delimitation that the decomposition/ reformation of ettringite started only if the sample weight loss/ gain exceeded 1% in 24 h ~~under the according experimental condition~~. Under low fixed vapour pressures, typically at 800 Pa, the water molecule number per formula dropped from 30.2 to 10.2 with temperature up to about 60 °C. Meanwhile, the crystallinity of ettringite reduced digressively according to XRD patterns. Same results were reproduced at a higher P_{H2O} while the temperature of dehydration to arrive an approximate water content must go higher, such as 95 °C for 4666 Pa and 105 °C for 5.3×10^4 Pa to attain n=13. The discussion of the stability of ettringite under different conditions was illustrated in **Fig. 5**.

At the left part of curves (zone of reformation), ettringite was both persistent and stable, which means that ettringite did not decompose, and the decomposed ettringite, meta-ettringite, would spontaneously recrystallize to ettringite. On the right of curves (zone of decomposition), the phenomenon was exactly contrary. The formula of meta-ettringite was said to be Met10-13 while Ett30-32 for ettringite. An important outcome of this study was that the reversible reaction occurred with a marked hysteresis (zone between curves). The reformation of

ettringite went under a relatively higher water vapour pressure compared with that of decomposition process. In the hysteresis zone, when starting from saturated water vapour pressures, crystal ettringite would not undergo decomposition unless the zone of decomposition is reached. Whereas, once decomposed, amorphous meta-ettringite would not reform to ettringite unless the zone of reformation was reached. ~~This mismatch may be due to the condensation of water on the surfaces and defects of amorphous phase at high relative humidity. Local nucleation of ettringite with liquid water will change the reformation mechanism.~~ Tambach et al. [76] proposed a fundamentally thermodynamic reason for ~~the~~ hysteresis phenomenon using molecular simulations: the hysteresis zone was somehow a free-energy barrier, which interrupted a continuous transition between two binomial hydrates. Thus, an increase or decrease in terms of humidity or temperature (or both) were necessary to overcome this barrier, which seems to be suitable for the transformation between ettringite and meta-ettringite [17].

Baquerizo et al. [17] also modelled the practical stability of ettringite under different conditions (**Fig. 6**) based on experimental results and theoretical extension by Van't Hoff equation. The general location of different zones and the curves agreed with former model [61], but differed below 60 °C, especially for reformation. Moreover, the theoretical thermodynamic curve of stability for ettringite and meta-ettringite has been plotted without hysteresis.

Thus, we can estimate that, at 25 °C, ettringite would reform from meta-ettringite when RH > 62%, whereas at 70 °C ettringite is said unstable at < 15% RH. The formula of ettringite considered as Ett30-32 on the curve of reformation while Met13 for meta-ettringite on the curve of decomposition. As a fact, these results were based on small quantity of ettringite powder~~s~~. So the removal process of water can be considered to occur under a constant condition without different local partial conditions in the samples. However, to a massive compact sample, the outcome could be very different [69]. On the other hand, seen from different investigations [17,38,57,59,61], intermediate products between ettringite and Met10-13 were existed, such as Met17.2, Met20.5, Met25.9, which were indistinguishable in the present modelling diagrams. As reason of the marked hysteresis, these partially dehydrated products are predicted to locate in a narrow zone around the curve of decomposition for dehydration process. Similarly, a narrow zone exists around the reformation curve for hydration process. ~~Thus~~ Therefore, it is probably difficult to definitely separate the different zones for each intermediate product, which may also explain why they were not stepwise

detectable in TGA or DSC with a typically high speed of scan temperature (10 °C/min) [17,27,36,77].

4.4. Thermal enthalpies of dehydration and hydration

With high water content and different chemical environment for water molecules in ettringite, the enthalpies of dehydration and hydration are related to the water content of initial and final hydrates. Meanwhile, the special heat capacity would also change in function of water content.

Ings and Brown [14] completed heat investigation on the reversible hydration reaction of ettringite, of which a "latent heat" of only 21 J/g was exhibited at 64 °C with sealed sample pans in DSC. However, with the temperature of dehydration rising up, the exothermic heat increased obviously, such as 405.8 J/g for 100 °C. The ~~indicated~~ thermal capacity of synthetic ettringite ~~from~~ indicated by Struble and Brown [15,16] was approximately 1.3 J/(g·K), which showed the little potential for sensible heat storage regarding 4.19 J/(g·K) for water. More importantly, they determined the enthalpy of chemical change of ettringite was about 600 J/g phase (decomposition occurred at temperature from 30 to 70 °C), which preliminarily showed the interest for thermal energy storage. ~~Compared with the enthalpy of vaporization of water (2257 J/g), this value (600 J/g, equals to 2100 J/g H_2O) is more rational if without probably existing mistakes in the analysis of results or in the measurements.~~ However, this value (600 J/g ettringite, equals to 2100 J/g H_2O) was thought unreasonable since it was smaller than the enthalpy of vaporization of water (2257 J/g H_2O) [17]. Otherwise, it means that the removal of water from crystal structure needs less energy than water evaporation. Jiménez and Prieto [36] demonstrated the different enthalpies of dehydration for natural and synthetic ettringite using TG and DSC: the natural one needed 2066 J/g for a removal of 23 water molecules per phase at 190 °C while the synthetic consumed 1498 J/g to release 19 molecules. In comparison to the investigation of Baquerizo et al. [17] (973.3 J/g for producing Met9.3 at 60 °C and 997.2 J/g for Met8.3 at 65 °C based on synthetic ettringite), these values were obviously higher. This may be due to the more perfect crystal structure or a higher crystallinity. Because the ~~decomposition~~ dehydration of crystal is partly controlled by the escaping rate of water, which means the size and perfectivity of crystal affect the penetration resistance for ~~vapour~~ water molecule and more energy is necessary to ~~break~~ overcome this ~~block~~ obstruction. Since the first report by Struble and Brown [15], some investigations on the energy storage capacity of ettringite have been realized. The principal ~~fruit is~~ results are summed up as following in **Table 5**:

642 **Table 5. Synthesis of different decomposition and rehydration reactions for ettringite**
643 **and their enthalpies**

Process	Reaction	ΔH (kJ/mol)	ΔH (kJ/mol H_2O)	Mass / Size of Samples (powder)	Reference
Dehydration	Ett32 (s)→ Met12 (s)+ 20H_2O(g)	+ 630	+ 31.5	~1 mg	[15]
		+ 1135*	+ 56.7*	/	[17]
	Ett32 (s)→ Met13 (s)+ 19H_2O(g)	+ 753 (±126)	+ 39.8 (±6.6)	~1 mg	[16]
		+ 1074*	+ 56.5*	/	[17]
	Ett31 (s)→ Met9.3 (s)+ 21.7H_2O(g)	+ 1204 (60 °C)	+ 55.5	5.53 mg	[17]
	Ett31(s)→ Met8.7 (s)+ 22.3H_2O(g)	+ 1233 (65 °C)	+ 55.2	8.93 mg	
	Ett (s)→ Met (s)+ 19H_2O(g)	+ 1878 (130 °C)	+ 98.8	~20 mg	[36]
Hydration	Met15.5 (s)+ 16.5H_2O (l)→ Ett32(s)	- 241	-14.6	Several grams	[15]
		- 205*	- 12.4*	/	[17]
	Met10.5 (s)+ 21.5H_2O (l)→ Ett32(s)	- 385	- 17.9	Several grams	[15]
		- 279*	- 13.0*	/	[17]
	Met11 (s)+ 21H_2O (l)→ Ett32(s)	-238.5	- 11.4	38 – 50 mg	[17]
	Met9 (s)+ 23H_2O (l) → Ett32(s)	- 286	- 12.4	492 mg	
	Met 9(s)+ 23H_2O (g) → Ett32(s)	- 1316.1	- 57.2	~80 mg	

644 *: Calculated values basing on a hydration process in calorimetry from [17].

645 Although the dehydration/ hydration processes are not identical, according to the number
646 of water molecules released/ gained, the promising future for the energy storage by ettringite
647 could still be seen clearly. There exists a distinct mismatch of enthalpy during the reversible
648 processes owing to the condensation of water ~~(about 40.8 kJ/mol)~~. Note that: if humid air is
649 used to hydrate meta-ettringite, ~~a same endothermic value~~ same amount of heat should be
650 theoretically released. However, the quantity of released heat during hydration process was
651 reported to have trends to reduce with the number of cycles (dehydration/ rehydration) going
652 up but no change for complete heat release time [14]. As indicated by Fopah-Lele and Tamba
653 [3], the hydration of most of the salt for energy storage underwent an inconsistent reversible
654 process. The stoichiometrically removed water from salt was insufficient to dissolve all solid
655 phase and re-crystallize salt crystal. This is similar to ettringite as a complex sulfate, which

could be seen more or less from the investigation [14]. The small enthalpy was very likely owing to the incomplete hydration by self-released water. Hence, two or more XRD-discernible solid phases (ettringite and lower hydrates) should exist at this transition point. Furthermore, unlike salts, the over-hydration (form a saturated solution, not a hydrate) caused by excessive water from humid air is not noticeable for ettringite thanks to its low dissolubility. Contrarily, the high humidity or pressure of water vapour may help to form a higher water content phase [57,59], which could release more heat by forming more "zeolithic waters".

5. Chemical stability of ettringite relating to thermal energy storage

5.1. Carbonation of ettringite

Calcium carbonate mineral is one of the main products for the carbonation of a cementitious material, which contains three polymorphs: aragonite, vaterite and calcite. Once a cementitious component carbonated, the process is irreversible cause of the relevantly lower Gibbs free energy of calcium carbonate than initial non-carbonated phases under ambient conditions. To ensure the reversibility of meta-ettringite approaches the initial point, alkaline phase need to be avoided any presence of active components including CO_2. As Robl et al. [78] stated, dry ettringite samples did not carbonate significantly under CO_2 environment, while contrary for hydrated ettringite. From this fact, the role of water in the carbonation of ettringite is important. But how does water severe in this process?

The dissolution of CO_2 in water releases H^+ ions and produces a slight acidic solution:

$$CO_2 + H_2O \leftrightarrow H^+ + HCO_3^- \quad K_a = 2.5 \times 10^{-4} \quad (15)$$

This solution can nearly attack all alkaline cement components, including ettringite. Generally, CO_2 can enter cement matrix by two ways: penetration by gas phase or diffusion by CO_3^{2-} ions from dissolution of CO_2 and from carbonate solid phases. The difference between a pore solution in cement matrix and pure water for the dissolution of CO_2 are [29]:

i. that CO_2 has a bigger solubility in an alkaline pore solution than other gases;
ii. that the solubility of CO_2 is influenced by pressure, pH and temperature;
iii. that the alkalinity promotes the solubility of CO_2 comparing with in neutral water.

Pajares and his coworkers [79] indicated the harmful effect of carbonate ions, respectively from $CaCO_3$ and $MgCO_3$ silica gel saturated solution, on structure of ettringite at ambient

686 temperature. But the presence of $Ca(OH)_2$ could evidently delay the carbonation of ettringite.
687 Same phenomenon caused by carbonate ions at different temperatures had been also reported
688 [80].

689 Detailed works by Grounds et al. [81] on the carbonation of ettringite described that
690 carbonation effect by atmospheric CO_2 was enhanced at increasing temperatures with a
691 constant humidity. According to XRD and TG analysis, the calculated variation of weight for
692 decomposition products suggested the carbonation reaction was:

693 $3CaO{\cdot}Al_2O_3{\cdot}3CaSO_4{\cdot}32H_2O + 3\ CO_2 \rightarrow 3\ CaSO_4{\cdot}2H_2O + 3\ CaCO_3 + 2\ Al(OH)_3 + 23\ H_2O$ (16)

694 This process was confirmed by other investigations [82,83]. Considering the quantity of
695 produced components during carbonation process, the mechanism could be described as two
696 stages [81]: First step was the one dimensional diffusion of CO_2, which agreed with the
697 relationship $\alpha^2=kt$ (**Eq. 17**[4]). In this stage, CO_2 diffused along the channels and broke the
698 charge balance at the column surface. Meanwhile CO_3^{2-} became competitive to SO_4^{2-}. And
699 ettringite crystal probably split, which initiated further reactions at created defects. The
700 corresponding equation for the second step was $1-(1-\alpha)^{1/3}=kt$ (**Eq. 18**). This process indicated
701 a controlled reaction by reducing area of reaction interface or reducing volume in cylindrical
702 or lath-like structures. During the second stage, carbonate penetrated into and along the
703 column material, which caused the disruption of main structure with rapid formation of
704 calcium sulfate, calcium carbonate and amorphous aluminium hydroxide.

705 Similarly, Nishikawa et al. [82] agreed that the carbonation process could be described by
706 two phases and proposed a following numerical relationship:

707 $$[1-(1-\alpha)^{1/3}]^N=kt \quad (19)$$

708 Where N was the index of the rate determining step: if N= 1, different from [81], the equation
709 suggested a dissolution step of CO_2 at the surface; if N=2, a diffusion controlled step through
710 product-layer was presented. In addition, at the final step of dry-condition (without pre-mixed
711 with water, but water were produced before by carbonation reaction) and through the whole
712 process of wet-condition (pre-mixed by w/s =3), the diffusion-controlled step (N=2) was
713 always predominant. However, their synthetic ettringite samples had been dried in a vacuum
714 of 0.4 Pa for 1 week. Under such condition, ettringite was supposed to ~~decompose~~ dehydrate

[4] α: decomposition proportion of ettringite; t: time; k: constant

to a lower hydrate [59], which still maintained main structure of ettringite crystal and distinguishable in XRD. This prediction was supported by the disappearance of large endothermic peak of ettringite in TG [82]. Detailed works by Chen et al. [83] integrated directly CO_2 partial pressure, water vapor pressure and temperature together (**Eq. 20**). The increase of CO_2 pressure (from 6660 to 40000 Pa) and of water vapor (27 - 1227 Pa) could obviously accelerate linearly the carbonation of ettringite. Moreover, effect of temperature at 10 – 50 °C was very important for the carbonation kinetic.

$$v = \frac{dx}{dt} = k_0 e^{39907/RT} P_{H2O} P_{CO2} \quad (20)$$

When under water vapor saturated state, the equation could be simplified to:

$$v = \frac{dx}{dt} = k_0' \, e^{-E_a/RT} P_{CO2} \quad (21)$$

Where v is the carbonation speed, x the carbonation rate, t the time of reaction (h), k_0 and k_0' the carbonation reaction rate constants, E_a the apparent activation energy, R the gas constant, T the temperature (K) of reaction and P_{H2O}, P_{CO2} for water vapour and CO_2 partial pressure (Pa) respectively.

The above carbonation kinetic (**Eq. 21**) was accompanied by following chemical mechanism:

$$H_2O + * \rightarrow H_2O* \quad (22)$$

$$H_2O* + CO_2 \rightarrow H_2CO_3* \quad (23)$$

$$H_2CO_3* + 1/3\ (3CaO{\cdot}Al_2O_3{\cdot}3CaSO_4{\cdot}32H_2O) \rightarrow CaCO_3 + CaSO_4{\cdot}2H_2O + 1/3\ Al_2O_3\ {\cdot}XH_2O + [1/3(29\text{-}X)\ \text{-}1]\ H_2O + H_2O* \quad (24)$$

Where * was the active center. In this process, H_2O was not reactive but could attend the carbonation process like a catalyst. Moreover, the CO_2 capture step was the rate determining step. Therefore, θ_{H2CO3} was much smaller than θ_{H2O}[5].

Developed from the above investigations on ettringite powders, carbonation experiments on pellets (2.5 mm thick) pressed to about 80% theoretical density with parallel carbonation study on pure ettringite powder (< 250 µm) were ~~preliminarily~~ executed by Zhou and Glasser

[5] θ presents the fraction of reactive component.

[84]. The observed acceleration of carbonation on powder samples with both increasing relative humidity and temperature was in good agreement with [83]. Inconsistent with powder samples, compacted pellets gave additionally AFm phase since the condensation of water in the pores and inter-crystal space. Additionally, the quantity of condensation water depended on pore geometry and pore volume. Another important outcome of this report was the study on the evolution of carbonation products with depth up in the pellets, shown in **Fig. 7**.

As a product of carbonation, the liberated water made the pore space flooded in the reactive layer reducing geometric contact surface of CO_3^{2-}-water interface and disfavored the carbonation process. Considering slower escape of water in pellets than in loose powder, a water rich zone was supposed to form between zone III and IV (dot zone). This could explain the nucleation and crystallization of AFm, which matched well with the thermal decomposition of ettringite at 100% RH or in water. However, the remained AFt phase may already contain carbonate structure said to be recognizable through the slight shift of diffraction peak in XRD patterns as described by Hirabayashi et al. [85]. Same interpretation was also referred via FTIR spectra analyses for synthetic ettringite [19,43]. Damidot and Glasser [86] proved that CO_3^{2-} ions had great possibility to substitute into AFt phases, especially at the boundaries of the stability zone of ettringite (**Fig. 8,** a-b-h-g-f) through the calculation for the stability of ettringite in CaO-Al_2O_3-$CaSO_4$-$CaCO_3$-H_2O system at 25 °C.

An ettringite based material, CSA cement paste powder (63 μm), ha~~ds~~ been recently examined under 4% CO_2 at 25 °C and 65% RH [23]. After exposure for 10 days, 71% ettringite ~~had been~~ was carbonated to hemihydrate, amorphous aluminium hydroxide and calcium carbonate (aragonite and vaterite) without the formation of AFm as reported before. On the other hand, as the binomial of ettringite, the carbonation resistance and corresponding mechanism are still barely discussed in detail for meta-ettringite. However, there is no doubt that ettringite is needed to be protected from CO_2 if used as an energy storage material.

5.2. Ionic substitution phenomenon

Due to the capacity of co-existing with substitutes in crystal structure, whether partial or total, ettringite was considered as a good host phase [87]. Some substitutions exist in nature while others are synthesizable or presumed basing on electronic charge balance and similar ion radius (Table 6). Exchanges can be made with cations and anions, such as chromate, arsenate [88] or selenate [89] for sulfate; lead, cadmium, cobalt for calcium [90] and iron, chromium for aluminium [15]. Tashiro et al. [91] reported that some heavy metal oxides and

hydroxides, like Cr_2O_3, Fe_2O_3, $Cu(OH)_2$, ZnO and $Pb_2O(OH)_2$ promoted the crystal growth of ettringite and produced some changes in microstructure by adding 5 % by weight of above additives. Morphology of these ettringites was almost identical and no evident difference showed in XRD patterns [29].

Coordination, size, and electronegativity were likely the principal indicators that result in the observed differences among the oxyanions. These substitution phenomena most probably occurred by the reason of that, those particle surfaces of ettringite exhibited a net negative charge [92]. Therefore, incorporation of anions in the bulk is much more important than surface adsorption. The extent of solid solution with ettringite was thought to be inversely proportional to the difference in size and electronegativity of the oxyanion compared with SO_4^{2-} [93]. Thus, the uptake of MoO_4^{2-} was ignorable or even non-existent, which could be attributed to a large size and made it unstable. However, solid solution is probably determined by more factors than just size and electronegativity. Ettringite showed amity to CrO_4^{2-} and SeO_4^{2-}, of which substituted ettringite reflected a similar solubility compared with a pure one [94]. Kumarathasan et al. [95] also had synthesized X-ray diffraction phase pure products with chromate and selenate, substituted completely sulfate in ettringite, and with partial substitution for arsenate, borate and vanadate. Zhang and Reardon [96] established the removal of B, Cr, Mo, and Se oxyanions from high pH waters by incorporation into ettringite. Else, ettringite showed an anion affinity in the order of $B(OH)_4^- > SeO_4^{2-} > CrO_4^{2-} > MoO_4^{2-}$, which corresponded to the work of [93]. Borate was verified as an oxyanion to incorporate easily into ettringite with supporting of the existence of several natural borate-substituted ettringite [97]. However, SO_4^{2-} was still preferable to form ettringite than other ions like SeO_4^{2-} [89]. Therefore, the formation of ettringite follows this affinity order when diverse oxyanions present in a mixed solution. Equally, CO_3^{2-}-, IO_3^{2-}-, Cl^--ettringite had also been reported [14,15,98]. It seems thus reasonable to hypothesize that, a partially or completely substituted ettringite would contain two or more types of oxyanion in a mixed solution without adequate sulfate ions supply.

The competing effects in ettringite are reported not only for anions but also for cations to replace aluminium and calcium in the column structures. Respecting to electron balance, Al was possible to be replaced by Ti^{3+}, Ga^{3+}, Cr^{3+}, Mn^{4+}, Si^{4+}, Fe^{3+} or Ge^{4+}, and Ca^{2+} by Sr^{2+} or Pb^{2+} [99]. Some nature minerals containing cation substitutes are also well known as

members of ettringite group. Among them, thaumasite and jouravkite[6] have close a-axial length compared with ettringite. Synthesis of naturally existing Cr^{3+}-ettringite, which owned similar properties with ettringite has been respectively reported by several investigations [15,34]. A structural model for Sn^{4+} uptake by ettringite was developed based on the crystallographic parameters. Preliminary experiments further supported that ettringite could be a host phase for Sn^{4+} even without respect to equal electric exchange to Al^{3+} [100]. Similarly, Si^{4+}, Ge^{4+} and Mn^{4+} have been equally mentioned to replace Al^{3+} in [99].

Table 6. Total or partial ionic substitutions in the structure of ettringite basing on detailed work from[14,15,87,88,90,94,96,97,99,101–112].

Replaced ion	Acceptable ionic size (Å)	Total or partial substitution		
		Natural existing	Obtained by synthesis	Suspected but unproven
Ca^{2+}	0.90 – 1.42	/	Cd^{2+}, Sr^{2+}	Co^{2+}, Ni^{2+}, Ba^{2+}, Pb^{2+}, Mg^{2+}, Mn^{2+}, Cu^{2+}, Zn^{2+}
Al^{3+}	0.42 – 0.76	Si^{4+}, Fe^{3+}, Cr^{3+}, Mn^{3+}	Ti^{3+}	Ni^{3+}, Co^{3+}, Ga^{3+}
SO_4^{2-}	0.62 – 3.71	$B(OH)_4^-$, CO_3^{2-}, SO_3^{2-}	OH^-, Cl^-, I^-, MoO_4^-, CrO_4^{2-}, SeO_4^{2-}, SeO_3^{2-}, VO_4^{3-}, AsO_4^{3-}, $HCOO^-$	BrO_3^-, ClO_3^-, IO_3^-, NO_3^-
OH^-	0.62 – 1.38	/	/	O^{2-}

In fact, most substituted ettringite probably share analogous physical and chemical properties, which account on their similar structures such as solubility, alkalinity, and large water content. Struble and Brown [15] studied thermal dehydration properties on several substituted ettringite and found that the measured enthalpies were ranged between 418 joules and 962 joules per gram of sample. For example, a Fe-substituted ettringite lost more H_2O molecules and had a bigger thermal decomposition enthalpy (800 J/g) than a normal ettringite (600±100 J/g) under same condition [16]. If considering differently, the enthalpies of removing per mole of water were respectively ~~close (~~37.8 kJ/mol H_2O for ettringite and 46.8 kJ/mol H_2O for Fe-substituted ettringite~~)~~. ~~Reversibly~~ Besides, Fe-substituted ettringite could also sustain dehydration and hydration loops but with a diminution of liberated heat (about 56% lower than that of normal ettringite) [14]. Antao et al. [27] reported that the dehydration of sturmanite (ideal empirical formula: $4CaO{\cdot}Fe_2O_3{\cdot}0.5B_2O_3{\cdot}2CaSO_4{\cdot}33H_2O$) at 150 °C gave an enthalpy of 1660 J/g with 41.6% weight loss (28.7 H_2O) while 641 J/g for ettringite of 40.4% loss (26.6 H_2O) at 170 °C. Kumarathasan et. al [95] investigated the heat of dehydration for a

[6] Thaumasite: $Ca_6[Si(OH)_6]_2{\cdot}24H_2O\}(SO_4)_2(CO_3)_2$ and jouravkite: $Ca_6[Mn(OH)_6]_2{\cdot}24H_2O\}(SO_4)_2(CO_3)_2$

series of oxyanion substituted ettringite and the enthalpy value varied with the oxyanion ratio in per phase (Table 7).

Table 7. Dehydration heat for different oxyanion substituted ettringite from [95]

Oxyanion mole ration from chemical analysis [a]	Heat of dehydration [b] (J/g)	Weight loss [c] (wt%)	Possible corresponding theoretical formula of substituted ettringite
$(SO_4)_{3.3}$	600	45	$Ca_6Al_2(SO_4)_3(OH)_{12}\cdot 26H_2O$
$(SO_4)_{2.6}(AsO_4)_{0.3}$	830	45	$Ca_6Al_2(AsO_4)_2(OH)_{12}\cdot 26H_2O$
$(SO_4)_{3.0}[B(OH)_4]_{1.0}$	1180	45	$Ca_6Al_2(SO_4)_2[B(OH)_4](OH)_{12}\cdot 26H_2O$
$(SO_4)_{2.2}[B(OH)_4]_{1.2}$	1230	47	
$(SO_4)_{1.5}[B(OH)_4]_{1.4}$	1280	51	
$(SO_4)_{2.5}(CrO_4)_{0.6}$	840	47	$Ca_6Al_2(CrO_4)_3(OH)_{12}\cdot 26H_2O$
$(SO_4)_{2.7}(CrO_4)_{1.3}$	580	45	
$(CrO_4)_2$	470	39	
$(SO_4)_{2.8}(SeO_4)_{0.5}$	940	47	$Ca_6Al_2(SeO_4)_3(OH)_{12}\cdot 26H_2O$
$(SO_4)_{1.7}(SeO_4)_{1.2}$	880	46	
$(SeO_4)_{2.5}$	760	43	
$(SO_4)_{2.8}(VO_4)_{0.5}$	520	58	$Ca_6Al_2(VO_4)_2(OH)_{12}\cdot 26H_2O$

a: Normalized to 6 Ca.

b: For the endotherm with a maximum at 100 – 140 °C by DSC.

c: Loss on ignition at 850 °C for 18 hours.

They considered that the value of the $(SO_4)_{3.3}$ phase was indeed as same as that reported by Struble and Brown [15]. Basing on this indication, most of the oxyanion substituted ettringites got a higher dehydration heat than a normal one and the value depended on the substitution degree of sulphate. Furthermore, the $B(OH)_4^-$ phases demonstrated the largest dehydration heat and approximately doubled the one of a normal ettringite. It was said that this evident increase came from the whole stronger hydrogen bonds in the borates, which could be seen from FTIR study [95]. In addition, thaumasite could present a higher dehydration enthalpy (1215 J/g) than ettringite (930 J/g) in DSC (50 – 250 °C) [113].

With this understanding, some physical and chemical natures of ettringite may be modified by total or partial replacement of cations, anions or both. Especially for thermal properties, a divalent or trivalent metallic substitution can possibly change the chemical environment of combined water groups. Thermal performance is thereby changed by the modification of relevant chemical ~~bounds~~ bonds. Similarly, the modification by oxyanions

may also make ettringite more resistant from CO_2 because of having a smaller mobility for a substitute anion than CO_3^{2-}.

6. Conclusion

Despite that the use of ettringite for thermal energy storage has not been scooped deeply out, this comprehensive review synthesizes its relevant thermal properties, preparation methods, chemical durability, etc. In comparison to other materials for energy storage, such as zeolite, $MgSO_4$, NaOH, ettringite promises a theoretically higher rehydration enthalpy thanks to the larger water content. Giving that the lack of standards for acceptable prescribed minimum of phasic releasable energy and necessary thermo-physical properties to determine, the researches on ettringite are still insufficient for applications of storing heat. No identical enthalpies of thermal procedures and few studies on the prototypes of large volume have been reported. Moreover, technical problems facing on ~~thermal~~ heat exchangers, carbon-resistance and absorption ~~include~~ including the instability of adsorbent and variability of systems during rehydration/ dehydration processes increase uncertainty for big scale applications. In terms of the material itself, several unknowns and ~~variability~~ variabilities about ettringite need to be ~~cleared~~ clarified:

- ✓ Thermal conductivity and specific heat capacity with the reduction of water content in ettringite phase are supposed to be completed.
- ✓ The re-examination of enthalpies of dehydration and hydration under different conditions (temperatures, relative humidity) will ensure the energy performance; meanwhile, the capacity of reversibility should be examined in detail, not only for ettringite but ettringite based materials. In addition, the study on the change of lattice parameter of meta-ettringite during rehydration may be able to be meaningful.
- ✓ A foreign ~~ions~~ ion substituted ettringite may be able to be more adaptable to energy storage since the thermal properties and chemical resistance would be modified correspondingly. However, nearly all of recent investigations about substituted ettringite are focused on the ion immobilization. Their properties for energy storage are barely known.
- ✓ The already-known properties of ettringite are probably not adaptable for ettringite-based materials, which are mostly considered as cement materials. In these materials, ettringite is no longer a single phase and has the possibility to react with other compounds under certain conditions. Most investigations were executed on ettringite

powders, which minimize the effect of dynamic process. Thus, a very different result could be seen if the form of sample changes without mentioning the change of a chemical environment.

- ✓ Given that the preference of growing in a less stressed direction for ettringite crystal, new structures of ettringite-based materials may improve its mechanic performance while also enforce the penetration of water for rehydration, like an ettringite based aggregates porous concrete. Of course, the diffusion of CO_2 may be also strengthened. Therefore, the protection from CO_2 or regular replacement of material ~~in application~~ is necessary, which leads to care~~s~~ about the coordination between economy and systemic integration problems. On the other hand, a foreign ion substituted ettringite may also be an interesting ~~re~~solution for this problem.

Briefly, by making a general survey of the significant advance on thermochemical energy storage concept, the investigation on ettringite for energy storage seems to be insufficient. However, it can affirmatively make a follow-up and even surpass other actually existed materials in near future because of large capacity of storage and low cost by gaining from cementitious materials. This thermochemical storage concept based on ettringite will become~~s~~ a competitive technology with the development of material and system optimization.

7. Acknowledgements

The authors would like to appreciate Bruno Huet and Luis Guillermo Baquerizo Ibarra from LafargeHolcim R&D, for their respective meaningful discussions and advices about carbonation of cementitious materials and thermal conversion between ettringite and meta-ettringite.

8. References

[1] S. Hongois, F. Kuznik, P. Stevens, J.-J. Roux, Development and characterisation of a new $MgSO_4$–zeolite composite for long-term thermal energy storage, Sol. Energy Mater. Sol. Cells. 95 (2011) 1831–1837. https://doi.org/10.1016/j.solmat.2011.01.050.

[2] K. Johannes, F. Kuznik, J.-L. Hubert, F. Durier, C. Obrecht, Design and characterisation of a high powered energy dense zeolite thermal energy storage system for buildings, Appl. Energy. 159 (2015) 80–86. https://doi.org/10.1016/j.apenergy.2015.08.109.

[3] A. Fopah-Lele, J.G. Tamba, A review on the use of $SrBr_2 \cdot 6H_2O$ as a potential material for low temperature energy storage systems and building applications, Sol. Energy Mater. Sol. Cells. 164 (2017) 175–187. https://doi.org/10.1016/j.solmat.2017.02.018.

[4] K.E. N'Tsoukpoe, T. Schmidt, H.U. Rammelberg, B.A. Watts, W.K.L. Ruck, A systematic multi-step screening of numerous salt hydrates for low temperature thermochemical energy storage, Appl. Energy. 124 (2014) 1–16. https://doi.org/10.1016/j.apenergy.2014.02.053.

[5] B. Kilkis, S. Kakaç, Energy storage systems, Kluwer Academic Publishers Series E: Applied Sciences, 167 (1989) 311.

[6] L.F. Cabeza, A. Solé, C. Barreneche, Review on sorption materials and technologies for heat pumps and thermal energy storage, Renew. Energy. 110 (2017) 3–39. https://doi.org/10.1016/j.renene.2016.09.059.

[7] K.E. N'Tsoukpoe, N. Mazet, P. Neveu, The concept of cascade thermochemical storage based on multimaterial system for household applications, Energy Build. 129 (2016) 138–149. https://doi.org/10.1016/j.enbuild.2016.07.047.

[8] J. Stark, K. Bollmann, Delayed ettringite formation in concrete, Nord. Concr. Res. 23 (2000) 4–28.

[9] M.D. Cohen, Theories of expansion in sulfoaluminate - type expansive cements: Schools of thought, Cem. Concr. Res. 13 (1983) 809–818. doi:10.1016/0008-8846(83)90082-0.

[10] J. Bizzozero, C. Gosselin, K.L. Scrivener, Expansion mechanisms in calcium aluminate and sulfoaluminate systems with calcium sulfate, Cem. Concr. Res. 56 (2014) 190–202. https://doi.org/10.1016/j.cemconres.2013.11.011.

[11] D.Y. Yang, R. Guo, Experimental study on modulus and hardness of ettringite, Exp. Tech. 38 (2014) 6–12. doi:10.1111/j.1747-1567.2011.00744.x.

[12] D.D. Walker, T.B. Hardy, D.C. Hoffman, D.D. Stanley, Innovations and uses for lime, in: ASTM, 1992.

[13] J. Lehmann, Über den Ettringit, ein neues Mineral in Kalkeinschlüssen der Lava von Ettringen (Laacher Gebiet), Neues Jahrb. Für Mineral. Geol. Und Paläontologie. (1874) 273–275.

[14] J.B. Ings, P.W. Brown, An evaluation of hydrated calcium aluminate compounds as energy storage media, NASA STI/Recon Tech. Rep. N. 83 (1982).

[15] L.J. Struble, P.W. Brown, Evaluation of ettringite and related compounds for use in solar energy storage, Prog. Rep. Natl. Bur. Stand. Washington, DC. Cent. Build. Technol. (1984).

[16] L.J. Struble, P.W. Brown, Heats of dehydration and specific heats of compounds found in concrete and their potential for thermal energy storage, Sol. Energy Mater. 14 (1986) 1–12. https://doi.org/10.1016/0165-1633(86)90008-0.

[17] L.G. Baquerizo, T. Matschei, K.L. Scrivener, Impact of water activity on the stability of ettringite, Cem. Concr. Res. 79 (2016) 31–44. https://doi.org/10.1016/j.cemconres.2015.07.008.

[18] T. Grounds, H.G. Midgley, D. V Nowell, The use of thermal methods to estimate the state of hydration of calciumtrisulphoaluminate hydrate $3CaO{\cdot}Al_2O_3{\cdot}3CaSO_4{\cdot}nH_2O$, Thermochim. Acta. 85 (1985) 215–218. https://doi.org/10.1016/0040-6031(85)85567-2.

[19] R.B. Perkins, C.D. Palmer, Solubility of ettringite ($Ca_6[Al(OH)_6]_2(SO_4)_3{\cdot}26H_2O$) at 5–75°C, Geochim. Cosmochim. Acta. 63 (1999) 1969–1980. https://doi.org/10.1016/S0016-7037(99)00078-2.

[20] D.K. Sahoo, R. Mishra, H. Singh, N. Krishnamurthy, Determination of thermodynamic stability of lanthanum chloride hydrates ($LaCl_3 \cdot xH_2O$) by dynamic transpiration method, J. Alloys Compd. 588 (2014) 578–584. https://doi.org/10.1016/j.jallcom.2013.11.115.

[21] J. Kaufmann, F. Winnefeld, Cement-based chemical energy stores, Pat. EP 2576720 B1. (2011).

[22] M. Cyr, S. Ginestet, K. Ndiaye, Energy storage/withdrawal system for a facility, Pat. WO 2017089698 A1. (2015).

[23] K. Ndiaye, M. Cyr, S. Ginestet, Durability and stability of an ettringite-based material for thermal energy storage at low temperature, Cem. Concr. Res. 99 (2017) 106–115. https://doi.org/10.1016/j.cemconres.2017.05.001.

[24] K. Ndiaye, S. Ginestet, M. Cyr, Modelling and experimental study of low temperature energy storage reactor using cementitious material, Appl. Therm. Eng. 110 (2017) 601–615. https://doi.org/10.1016/j.applthermaleng.2016.08.157.

[25] K. Ndiaye, S. Ginestet, M. Cyr, Experimental evaluation of two low temperature energy storage prototypes based on innovative cementitious material, Appl. Energy. 217 (2018) 47–55. https://doi.org/10.1016/j.apenergy.2018.02.136.

[26] K. Ndiaye Stéphane;Cyr,Martin, Thermal energy storage based on cementitious materials: A review, AIMS Energy. 6 (2018) 97–120. http://dx.doi.org/10.3934/energy.2018.1.97.

[27] S.M. Antao, M.J. Duane, I. Hassan, DTA, TG, and XRD studies of sturmanite and ettringite, Can. Mineral. 40 (2002) 1403–1409. doi:10.2113/gscanmin.40.5.1403.

[28] A.S. Brykov, A.S. Vasil'ev, M. V Mokeev, Hydration of portland cement in the presence of aluminum-containing setting accelerators, Russ. J. Appl. Chem. 86 (2013) 793–801. doi:10.1134/S1070427213060013.

[29] F.P. Glasser, The stability of ettringite, in: Int. RILEM Work. Intern. Sulfate Attack Delayed Ettringite Form., RILEM Publications SARL, 2002: pp. 43–64.

[30] G. Renaudin, Y. Filinchuk, J. Neubauer, F. Goetz-Neunhoeffer, A comparative structural study of wet and dried ettringite, Cem. Concr. Res. 40 (2010) 370–375. https://doi.org/10.1016/j.cemconres.2009.11.002.

[31] T. Terai, A. Mikuni, Y. Nakamura, K. Ikeda, Synthesis of ettringite from portlandite suspensions at various Ca/Al ratios, Inorg. Mater. 43 (2007) 786–792. doi:10.1134/S0020168507070205.

[32] Y. Shimada, J.F. Young, Structural changes during thermal dehydration of ettringite, Adv. Cem. Res. 13 (2001) 77–81. doi:10.1680/adcr.2001.13.2.77.

[33] S. Mantellato, M. Palacios, R.J. Flatt, Impact of sample preparation on the specific surface area of synthetic ettringite, Cem. Concr. Res. 86 (2016) 20–28. https://doi.org/10.1016/j.cemconres.2016.04.005.

[34] R.B. Perkins, C.D. Palmer, Solubility of $Ca_6[Al(OH)_6]_2(CrO_4)_3 \cdot 26H_2O$, the chromate analog of ettringite; 5–75°C, Appl. Geochemistry. 15 (2000) 1203–1218. https://doi.org/10.1016/S0883-2927(99)00109-2.

[35] Y. Shimada, J.F. Young, Thermal stability of ettringite in alkaline solutions at 80°C, Cem. Concr. Res. 34 (2004) 2261–2268. doi:10.1016/j.cemconres.2004.04.008.

[36] A. Jiménez, M. Prieto, Thermal stability of ettringite exposed to atmosphere: Implications for the uptake of harmful ions by cement, Environ. Sci. Technol. 49 (2015) 7957–7964. doi:10.1021/acs.est.5b00536.

[37] H.F. Taylor, Cement chemistry, second ed., Thomas Telford, London, 1997.

[38] K. Ogawa, D.M. Roy, $C_4A_3\bar{S}$ hydration ettringite formation, and its expansion mechanism: I. expansion; Ettringite stability, Cem. Concr. Res. 11 (1981) 741–750. https://doi.org/10.1016/0008-8846(81)90032-6.

[39] E. Grusczscinski, P.W. Brown, J. V Bothe, The formation of ettringite at elevated temperature, Cem. Concr. Res. 23 (1993) 981–987. https://doi.org/10.1016/0008-8846(93)90052-B.

[40] Q. Zhou, E.E. Lachowski, F.P. Glasser, Metaettringite, a decomposition product of ettringite, Cem. Concr. Res. 34 (2004) 703–710. https://doi.org/10.1016/j.cemconres.2003.10.027.

[41] P.K. Mehta, A. Klein, Formation of ettringite by hydration of a system containing an anhydrous calcium sulfoaluminate, J. Am. Ceram. Soc. 48 (1965) 435–436. doi:10.1111/j.1151-2916.1965.tb14786.x.

[42] V. Šatava, O. Vepřek, Thermal decomposition of ettringite under hydrothermal conditions, J. Am. Ceram. Soc. 58 (1975) 357–359. doi:10.1111/j.1151-2916.1975.tb11513.x.

[43] G.Y. Pan, R.Q. Mao, J. Yuan, Research of dehydrated calcium sulphoaluminate hydrates (AFm) and its hydration, J Wuhan Univ Technol. 19 (1997) 28–30.

[44] J. Peng, Z. Lou, Study on the mechanism of ettringite formation, Journal-Chinese Ceram. Soc. 28 (2000) 511–515.

[45] P. Wencil Brown, P. LaCroix, The kinetics of ettringite formation, Cem. Concr. Res. 19 (1989) 879–884. https://doi.org/10.1016/0008-8846(89)90100-2.

[46] J. Havlica, S. Sahu, Mechanism of ettringite and monosulphate formation, Cem. Concr. Res. 22 (1992) 671–677. https://doi.org/10.1016/0008-8846(92)90019-R.

[47] F. Bannister, M. Hey, J. Bernal, Ettringite from Scawt Hill, Co. Antrim, Mineral. Mag. 24 (1936) 324–329.

[48] J. Murdoch, R.A. Chalmers, Ettringite ("Woodfordite") from Crestmore, California, Am. Mineral. 45 (1960) 1275–1278.

[49] A.E. Moore, H.F.W. Taylor, Crystal structure of ettringite, Nature. 218 (1968) 1048. http://dx.doi.org/10.1038/2181048a0.

[50] A.E. Moore, H.F.W. Taylor, Crystal structure of ettringite, Acta Crystallogr. Sect. B. 26 (1970) 386–393. doi:10.1107/S0567740870002443.

[51] S.M. Clark, B. Colas, M. Kunz, S. Speziale, P.J.M. Monteiro, Effect of pressure on the crystal structure of ettringite, Cem. Concr. Res. 38 (2008) 19–26. https://doi.org/10.1016/j.cemconres.2007.08.029.

[52] R. Berliner, M. Popovici, K.W. Herwig, M. Berliner, H.M. Jennings, J.J. Thomas, Quasielastic neutron scattering study of the effect of water-to-cement ratio on the hydration kinetics of tricalcium silicate, Cem. Concr. Res. 28 (1998) 231–243. https://doi.org/10.1016/S0008-8846(97)00260-3.

[53] M.R. Hartman, R. Berliner, Investigation of the structure of ettringite by time-of-flight

neutron powder diffraction techniques, Cem. Concr. Res. 36 (2006) 364–370. https://doi.org/10.1016/j.cemconres.2005.08.004.

[54] F. Goetz-Neunhoeffer, J. Neubauer, Refined ettringite ($Ca_6Al_2(SO_4)_3(OH)_{12}\cdot 26H_2O$) structure for quantitative X-ray diffraction analysis, Powder Diffr. 21 (2006) 4–11. doi: 10.1154/1.2146207.

[55] D. McConnell, J. Murdoch, Crystal chemistry of ettringite, Mineral. Mag. 33 (1962) 59–64. doi:10.1180/minmag.1962.033.256.09.

[56] A. Bezjak, I. Jelenic, Crystal structure investigation of calcium aluminium sulphate hydrate-ettringite, Croat. Chem. ACTA. 38 (1966) 239.

[57] N.N. Skoblinskaya, K.G. Krasilnikov, Changes in crystal structure of ettringite on dehydration. 1, Cem. Concr. Res. 5 (1975) 381–393. https://doi.org/10.1016/0008-8846(75)90093-9.

[58] C. Hall, P. Barnes, A.D. Billimore, A.C. Jupe, X. Turrillas, Thermal decomposition of ettringite $Ca_6[Al(OH)_6]_2(SO_4)_3\cdot 26H_2O$, J. Chem. Soc. Faraday Trans. 92 (1996) 2125–2129. doi:10.1039/FT9969202125.

[59] N.N. Skoblinskaya, K.G. Krasilnikov, L. V Nikitina, V.P. Varlamov, Changes in crystal structure of ettringite on dehydration. 2, Cem. Concr. Res. 5 (1975) 419–431. https://doi.org/10.1016/0008-8846(75)90017-4.

[60] M.R. Hartman, S.K. Brady, R. Berliner, M.S. Conradi, The evolution of structural changes in ettringite during thermal decomposition, J. Solid State Chem. 179 (2006) 1259–1272. https://doi.org/10.1016/j.jssc.2006.01.038.

[61] Q. Zhou, F.P. Glasser, Thermal stability and decomposition mechanisms of ettringite at <120°C, Cem. Concr. Res. 31 (2001) 1333–1339. https://doi.org/10.1016/S0008-8846(01)00558-0.

[62] W. Lieber, Ettringite formation at elevated temperatures, Cem. Kalk-Gips. 9 (1963) 364–365.

[63] C.J. Warren, E.J. Reardon, The solubility of ettringite at 25°C, Cem. Concr. Res. 24 (1994) 1515–1524. https://doi.org/10.1016/0008-8846(94)90166-X.

[64] P.K. Mehta, Stability of ettringite on heating, J. Am. Ceram. Soc. 55 (1972) 55–57. doi:10.1111/j.1151-2916.1972.tb13403.x.

[65] V.I. Babushkin, O.P. Mchedlov-Petrossyan, G.M. Matveyev, Thermodynamics of silicates, Springer, 1984.

[66] I. Nerád, S. Šaušová, L. Števula, The $CaO\text{-}Al_2O_3\text{-}CaSO_4\text{-}H_2O$ system equilibrium states, Cem. Concr. Res. 24 (1994) 259–266. doi:10.1016/0008-8846(94)90051-5.

[67] D. Damidot, F.P. Glasser, Thermodynamic investigation of the $CaO\text{-}Al_2O_3\text{-}CaSO_4\text{-}H_2O$ system at 50°C and 85°C, Cem. Concr. Res. 22 (1992) 1179–1191. https://doi.org/10.1016/0008-8846(92)90047-Y.

[68] D. Damidot, F.P. Glasser, Thermodynamic investigation of the $CaO\text{-}Al_2O_3\text{-}CaSO_4\text{-}H_2O$ system at 25°C and the influence of Na_2O, Cem. Concr. Res. 23 (1993) 221–238. https://doi.org/10.1016/0008-8846(93)90153-Z.

[69] J. Kaufmann, F. Winnefeld, B. Lothenbach, Stability of ettringite in CSA cement at elevated temperatures, Adv. Cem. Res. 28 (2016) 251–261. doi:10.1680/jadcr.15.00029.

[70] J. Pourchez, F. Valdivieso, P. Grosseau, R. Guyonnet, B. Guilhot, Kinetic modelling of

1086 the thermal decomposition of ettringite into metaettringite, Cem. Concr. Res. 36 (2006)
1087 2054–2060. https://doi.org/10.1016/j.cemconres.2006.06.007.

1088 [71] S. Abo-El-Enein, S. Hanafi, E. Hekal, Thermal and physiochemical studies on
1089 ettringite II: dehydration and thermal stability, Cemento. 85 (1988) 121–132.

1090 [72] K. Ogawa, D.M. Roy, $C_4A_3\bar{S}$ hydration, ettringite formation, and its expansion
1091 mechanism: II. Microstructural observation of expansion, Cem. Concr. Res. 12 (1982)
1092 101–109. https://doi.org/10.1016/0008-8846(82)90104-1.

1093 [73] E.E. Hekal, S.A. Abo-El-Enein, Effect of compression on microstructure and thermal
1094 stability of ettringite, in: Proc. 8th Int. Conf. Cem. Microsc., Orlando, FL, USA, 1986:
1095 pp. 227–243.

1096 [74] H. Pollmann, Characterization of different water contents of ettringite and kuzelite, in:
1097 Proc. 12th Int. Congr. Chem. Cem. Montr. Canada, 2007.

1098 [75] K. Kira, Y. Makino, Y. Murata, Dehydration and rehydration of ettringite, Gypsum
1099 Lime. 1981 (1981) 7–13. doi:10.11451/mukimate1953.1981.7.

1100 [76] T.J. Tambach, P.G. Bolhuis, B. Smit, A molecular mechanism of hysteresis in clay
1101 swelling, Angew. Chemie. 116 (2004) 2704–2706. doi:10.1002/ange.200353612.

1102 [77] D.G. Grier, E.L. Jarabek, R.B. Peterson, L.E. Mergen, G.J. McCarthy, Rietveld
1103 structure refinement of carbonate and sulfite ettringite, Adv. X-Ray Anal. 45 (2002)
1104 194–199.
1105 http://citeseerx.ist.psu.edu/viewdoc/download?doi=10.1.1.296.2092&rep=rep1&type=p
1106 df.

1107 [78] T.L. Robl, U.M. Graham, D.N. Taulbee, The effect of carbonation reactions on the
1108 long term stability of products made from dry FGD materials, in: Prepr. Pap. Am.
1109 Chem. Soc. Div. Fuel Chem., United States, 1996.

1110 [79] I. Pajares, S. Martínez-Ramírez, M.T. Blanco-Varela, Evolution of ettringite in
1111 presence of carbonate, and silicate ions, Cem. Concr. Compos. 25 (2003) 861–865.
1112 https://doi.org/10.1016/S0958-9465(03)00113-6.

1113 [80] P.M. Carmona-Quiroga, M.T. Blanco-Varela, Ettringite decomposition in the presence
1114 of barium carbonate, Cem. Concr. Res. 52 (2013) 140–148.
1115 https://doi.org/10.1016/j.cemconres.2013.05.021.

1116 [81] T. Grounds, H. G Midgley, D. V Novell, Carbonation of ettringite by atmospheric
1117 carbon dioxide, Thermochim. Acta. 135 (1988) 347–352. https://doi.org/10.1016/0040-
1118 6031(88)87407-0.

1119 [82] T. Nishikawa, K. Suzuki, S. Ito, K. Sato, T. Takebe, Decomposition of synthesized
1120 ettringite by carbonation, Cem. Concr. Res. 22 (1992) 6–14.
1121 https://doi.org/10.1016/0008-8846(92)90130-N.

1122 [83] X. Chen, R. Zou, X. Chen, Kinetic study of ettringite carbonation reaction, Cem. Concr.
1123 Res. 24 (1994) 1383–1389. https://doi.org/10.1016/0008-8846(94)90123-6.

1124 [84] Q. Zhou, F.P. Glasser, Kinetics and mechanism of the carbonation of ettringite, Adv.
1125 Cem. Res. 12 (2000) 131–136. doi:10.1680/adcr.2000.12.3.131.

1126 [85] D. Hirabayashi, K. Sawada, Y. Enokida, A. Hertz, F. Frizon, F. Charton, F. Brouno, F.
1127 Bagnols-sur-Ceze, Carbonation behavior of pure cement hydrates under supercritical
1128 carbon dioxide conditions–12199, in: WM Symposia, 1628 E. Southern Avenue, Suite
1129 9-332, Tempe, AZ 85282 (United States), 2012.

[86] D. Damidot, F.P. Glasser, Thermodynamic investigation of the CaO-Al_2O_3- $CaSO_4$-$CaCO_3$-H_2O closed system at 25°C and the influence of Na_2O, Adv. Cem. Res. 7 (1995) 129–134. doi:10.1680/adcr.1995.7.27.129.

[87] M. Dhoury, Influence of lithium and boron ions on calcium sulfoaluminate cement hydration : application for the conditioning of boron ion exchange resins, Université Montpellier, 2015. https://tel.archives-ouvertes.fr/tel-01328183.

[88] W. Wang, Y. Shao, H. Hou, M. Zhou, Synthesis and thermodynamic properties of arsenate and sulfate-arsenate ettringite structure phases, PLoS One. 12 (2017) e0182160. https://doi.org/10.1371/journal.pone.0182160.

[89] B. Guo, K. Sasaki, T. Hirajima, Characterization of the intermediate in formation of selenate-substituted ettringite, Cem. Concr. Res. 99 (2017) 30–37. https://doi.org/10.1016/j.cemconres.2017.05.002.

[90] D. Bonen, S.L. Sarkar, The effects of simulated environmental attack on immobilization of heavy metals doped in cement-based materials, J. Hazard. Mater. 40 (1995) 321–335. https://doi.org/10.1016/0304-3894(94)00091-T.

[91] C. Tashiro, J. Oba, K. Akama, The effects of several heavy metal oxides on the formation of ettringite and the microstructure of hardened ettringite, Cem. Concr. Res. 9 (1979) 303–308. https://doi.org/10.1016/0008-8846(79)90122-4.

[92] S.C.B. Myneni, S.J. Traina, T.J. Logan, G.A. Waychunas, Oxyanion behavior in alkaline environments: Sorption and desorption of arsenate in ettringite, Environ. Sci. Technol. 31 (1997) 1761–1768. doi:10.1021/es9607594.

[93] G. Cornelis, C.A. Johnson, T. Van Gerven, C. Vandecasteele, Leaching mechanisms of oxyanionic metalloid and metal species in alkaline solid wastes: A review, Appl. Geochemistry. 23 (2008) 955–976. https://doi.org/10.1016/j.apgeochem.2008.02.001.

[94] W.A. Klemm, J.I. Bhatty, Fixation of heavy metals as oxyanion-substituted ettringites, Portland Cement Association New York, Skokie, IL USA, 2002.

[95] P. Kumarathasan, G.J. McCarthy, D.J. Hassett, D.F. Pflughoeft-Hassett, Oxyanion substituted ettringites: Synthesis and characterization; and their potential role in immobilization of As, B, Cr, Se and V, MRS Proc. 178 (1989) 83. doi:10.1557/PROC-178-83.

[96] M. Zhang, E.J. Reardon, Removal of B, Cr, Mo, and Se from wastewater by incorporation into hydrocalumite and ettringite, Environ. Sci. Technol. 37 (2003) 2947–2952. doi:10.1021/es020969i.

[97] G.J. McCarthy, D.J. Hassett, J.A. Bender, Synthesis, crystal chemistry and stability of ettringite, a material with potential applications in hazardous waste immobilization, MRS Proc. 245 (1991) 129. doi:10.1557/PROC-245-129.

[98] G. Möschner, B. Lothenbach, J. Rose, A. Ulrich, R. Figi, R. Kretzschmar, Solubility of Fe–ettringite ($Ca_6[Fe(OH)_6]_2(SO_4)_3 \cdot 26H_2O$), Geochim. Cosmochim. Acta. 72 (2008) 1–18. https://doi.org/10.1016/j.gca.2007.09.035.

[99] H.F.W. Taylor, Crystal structures of some double hydroxide minerals, Mineral. Mag. 39 (1973) 377–389. doi:10.1180/minmag.1973.039.304.01.

[100] I. Bonhoure, E. Wieland, A.M. Scheidegger, M. Ochs, D. Kunz, EXAFS study of Sn(IV) immobilization by hardened cement paste and calcium silicate hydrates, Environ. Sci. Technol. 37 (2003) 2184–2191. doi:10.1021/es020194d.

[101] M.L.D. Gougar, B.E. Scheetz, D.M. Roy, Ettringite and C-S-H Portland cement phases for waste ion immobilization: A review, Waste Manag. 16 (1996) 295–303. https://doi.org/10.1016/S0956-053X(96)00072-4.

[102] V. Albino, R. Cioffi, M. Marroccoli, L. Santoro, Potential application of ettringite generating systems for hazardous waste stabilization, J. Hazard. Mater. 51 (1996) 241–252. https://doi.org/10.1016/S0304-3894(96)01828-6.

[103] M. Atkins, F.P. Glasser, Application of portland cement-based materials to radioactive waste immobilization, Waste Manag. 12 (1992) 105–131. https://doi.org/10.1016/0956-053X(92)90044-J.

[104] R. Berardi, R. Cioffi, L. Santoro, Chemical effects of heavy metals on the hydration of calcium sulphoaluminate $4CaO_3 \cdot Al_2O_3 \cdot SO_3$, J. Therm. Anal. Calorim. 50 (1997) 393–400. doi:10.1007/BF01980499.

[105] M. Chrysochoou, D. Dermatas, Evaluation of ettringite and hydrocalumite formation for heavy metal immobilization: Literature review and experimental study, J. Hazard. Mater. 136 (2006) 20–33. https://doi.org/10.1016/j.jhazmat.2005.11.008.

[106] P.J. Dunn, D.R. Peacor, P.B. Leavens, J.L. Baum, Charlesite, a new mineral of the ettringite group, from Franklin, New Jersey, Am. Mineral. 68 (1983) 1033–1037. http://www.minsocam.org/ammin/AM68/AM68_1033.pdf.

[107] F.P. Glasser, L. Zhang, High-performance cement matrices based on calcium sulfoaluminate–belite compositions, Cem. Concr. Res. 31 (2001) 1881–1886. https://doi.org/10.1016/S0008-8846(01)00649-4.

[108] B. Guo, K. Sasaki, T. Hirajima, Selenite and selenate uptaken in ettringite: Immobilization mechanisms, coordination chemistry, and insights from structure, Cem. Concr. Res. 100 (2017) 166–175. https://doi.org/10.1016/j.cemconres.2017.07.004.

[109] D.J. Hassett, G.J. McCarthy, P. Kumarathasan, D. Pflughoeft-Hassett, Synthesis and characterization of selenate and sulfate-selenate ettringite structure phases, Mater. Res. Bull. 25 (1990) 1347–1354. https://doi.org/10.1016/0025-5408(90)90216-O.

[110] D.R. Peacor, P.J. Dunn, M. Duggan, Sturmanite, a ferric iron, boron analogue of ettringite, Can. Mineral. 21 (1983) 705–709. https://rruff-2.geo.arizona.edu/uploads/CM21_705.pdf.

[111] S. Peysson, J. Péra, M. Chabannet, Immobilization of heavy metals by calcium sulfoaluminate cement, Cem. Concr. Res. 35 (2005) 2261–2270. https://doi.org/10.1016/j.cemconres.2005.03.015.

[112] H. Pollmann, Capability of cement-itious materials in immobilization process of hazardous waste materials, in: Proc. 15th Internatio-Nal Conf. Cem. Microsc., 1993: pp. 108–126.

[113] M. Drábik, L. Gáliková, E. Scholtzová, E. Hadzimová, Thermoanalytical events and enthalpies of selected phases and systems of the chemistry and technology of concrete part I. Calcium-silicate-aluminate-sulfate hydrates, Ceram. - Silikáty. 58 (2014) 184–187.

Revised caption of figures

Fig. 1. A possible concept of charging mode (left) and discharging mode (right) of solar thermal energy storage by ettringite materials for a single-family house basing on [1].

Fig. 2. The formation of ettringite based on $C_4A_3\bar{S}$ at pH > 10.7 [46]. **Eq. 7** and **Eq. 8** were supposed to carry out in the liquid interlayer while **Eq. 9** in the solution of high pH.

Fig. 3. Section of ettringite unit structure (left): the polygons and the triangles represent respectively the main columns structure ($[Ca_6[Al(OH)_6]_2 \cdot 24H_2O]^{6+}$) and SO_4^{2-} or H_2O groups in channels [57]. Basic unit crystal structure of ettringite in c-axis direction (right): the O represents OH or H_2O group, while Al and Ca atoms are showed by chemical symbols [50,57].

Fig. 4. Hydrogen bonds network along *c*-axis (left) and perpendicular to *c*-axis (right) in ettringite crystal. Hydrogen bonds (light green) exist between column structure (water molecules and hydroxyls) and channel components (sulfate ions and water groups) providing the inter-column cohesion. The blue dashes represent O-D chemical bonds [53].

Fig. 5. Curves of the decomposition (right, equation of best fit $\ln P = -1.61 + 0.075T$) and reformation (left, equation of best fit $\ln P = 1.89 + 0.047T$) of ettringite as function of various water vapour pressures and temperatures based on experimental results. The numbers in the parentheses described the uncertainties of temperatures [62].

Fig. 6. Curves of reformation (left, equation of best fit: $RH = 56.608 + 0.186T + 0.001T^2$) and decomposition (right, equation of best fit: $RH = 0.327 + 0.108T - 0.002T^2 + 4.8\text{E-}5T^3$) as function of RH in **a)** or P_{H2O} in **b)** and temperature showing the separated zones. Dashed line represents the theoretical stability limit of ettringite [17].

Fig. 7. Schematic of layered zones developed spontaneously in carbonated ettringite pellets at 25–40°C and 68–88% RH. The sides and bottom were sealed to guarantee CO_2 and H_2O penetrate only from the top [85].

Fig. 8. Stability zones of ettringite as function of various sulfate and carbonate concentration of $CaO\text{-}Al_2O_3\text{-}CaSO_4\text{-}CaCO_3\text{-}H_2O$ system at 25 °C [29].

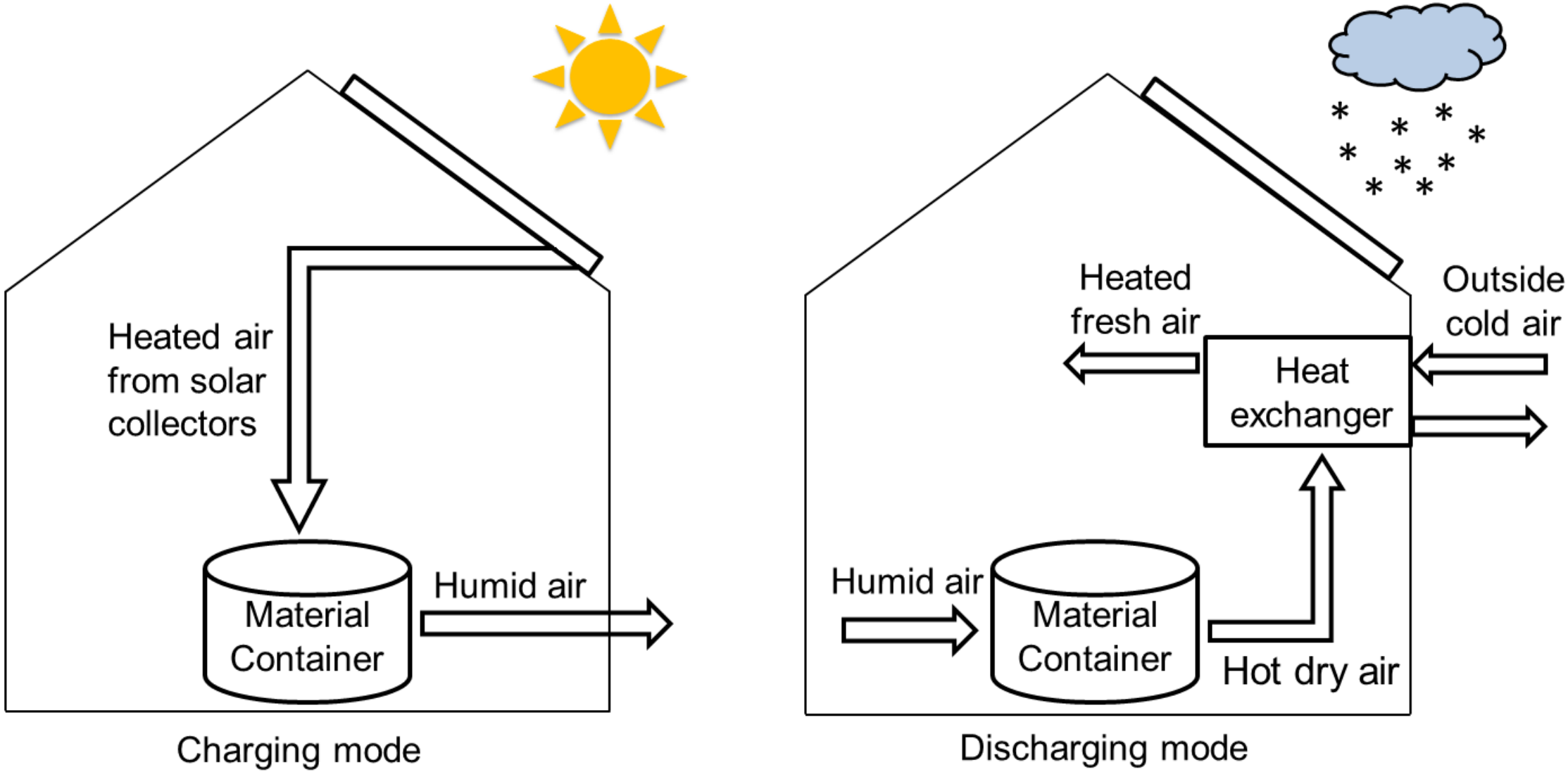
Heated air
from solar
collectors
Material
Container
Humid air
Charging mode
Heated
fresh air
Outside
cold air
Heat
exchanger
Humid air
Material
Container
Hot dry air
Discharging mode

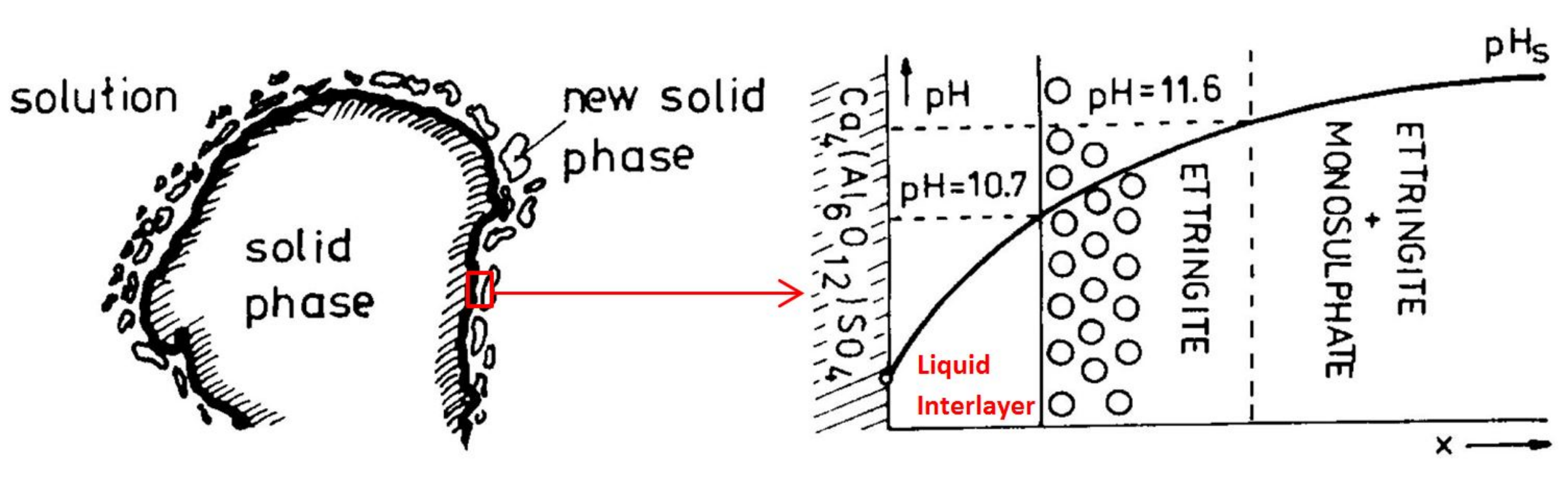
solution
new solid phase
solid phase
pH
pH=11.6
pH=10.7
pHs
Ca4(Al6O12)SO4
Liquid Interlayer
ETTRINGITE
MONOSULPHATE + ETTRINGITE
x

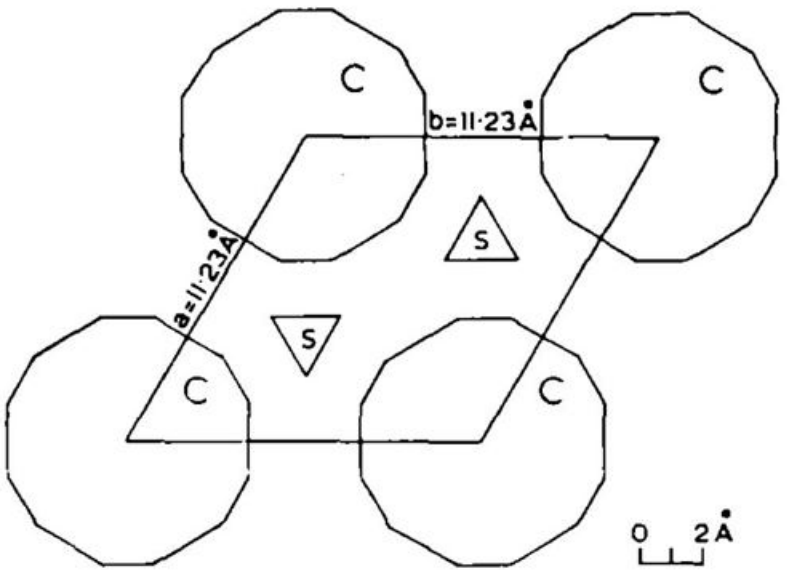
C
C
b=11·23Å
S
a=11·23Å
S
C
C
0 2Å

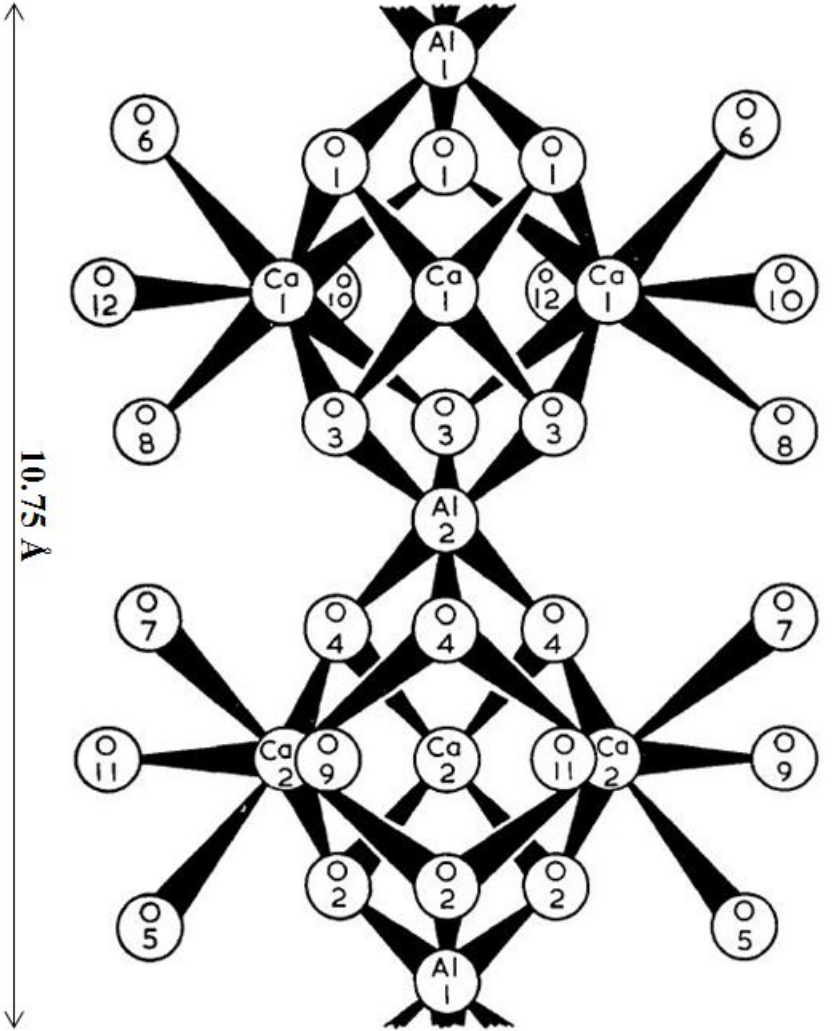
10.75 Å
Al 1
O 6
O 1
O 1
O 1
O 6
O 12
Ca 1
O 10
Ca 1
O 12
Ca 1
O 10
O 8
O 3
O 3
O 3
O 8
Al 2
O 7
O 4
O 4
O 4
O 7
O 11
Ca 2
O 9
Ca 2
O 11
Ca 2
O 9
O 2
O 2
O 2
O 5
O 5
Al 1

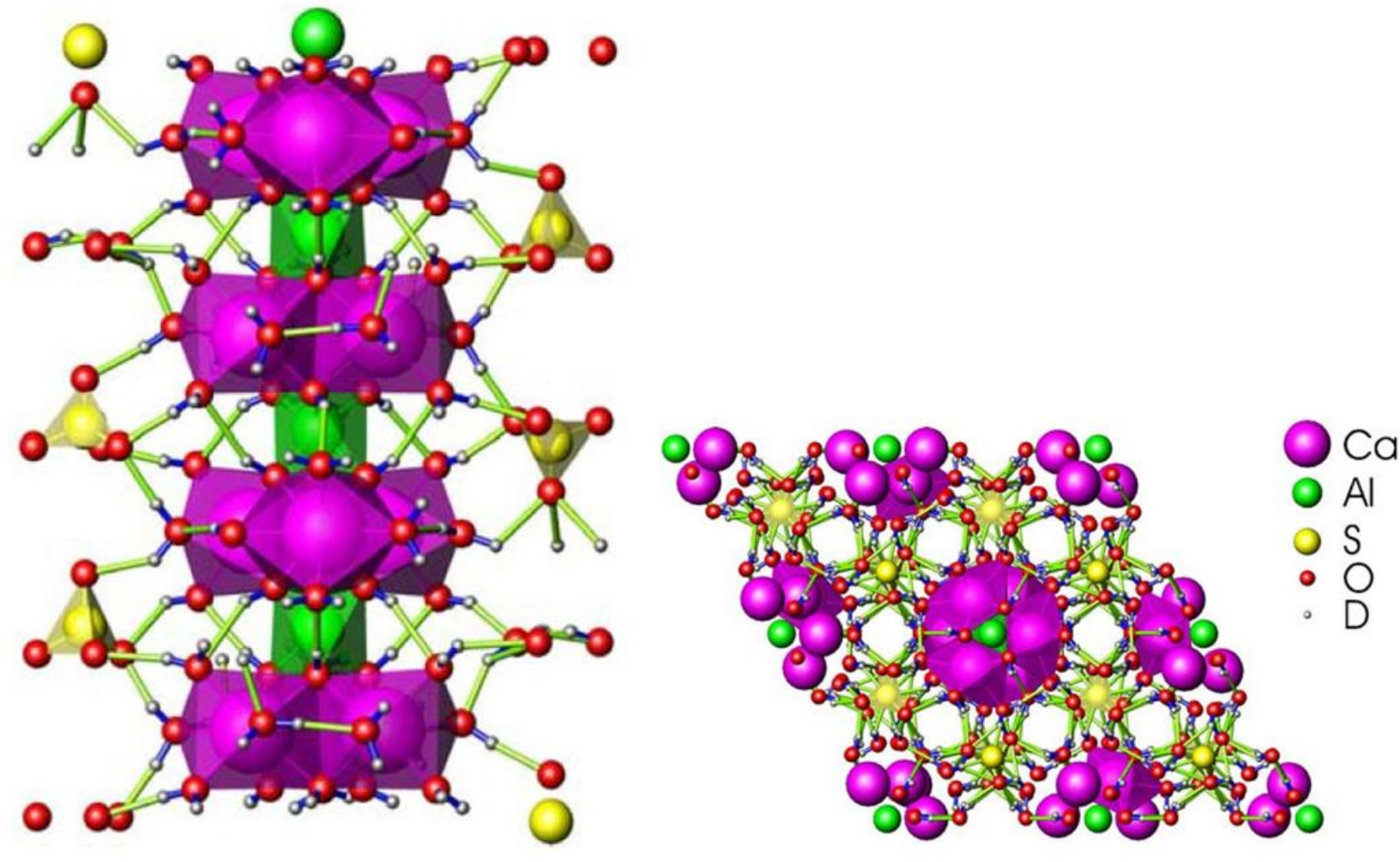
Ca
Al
S
O
D

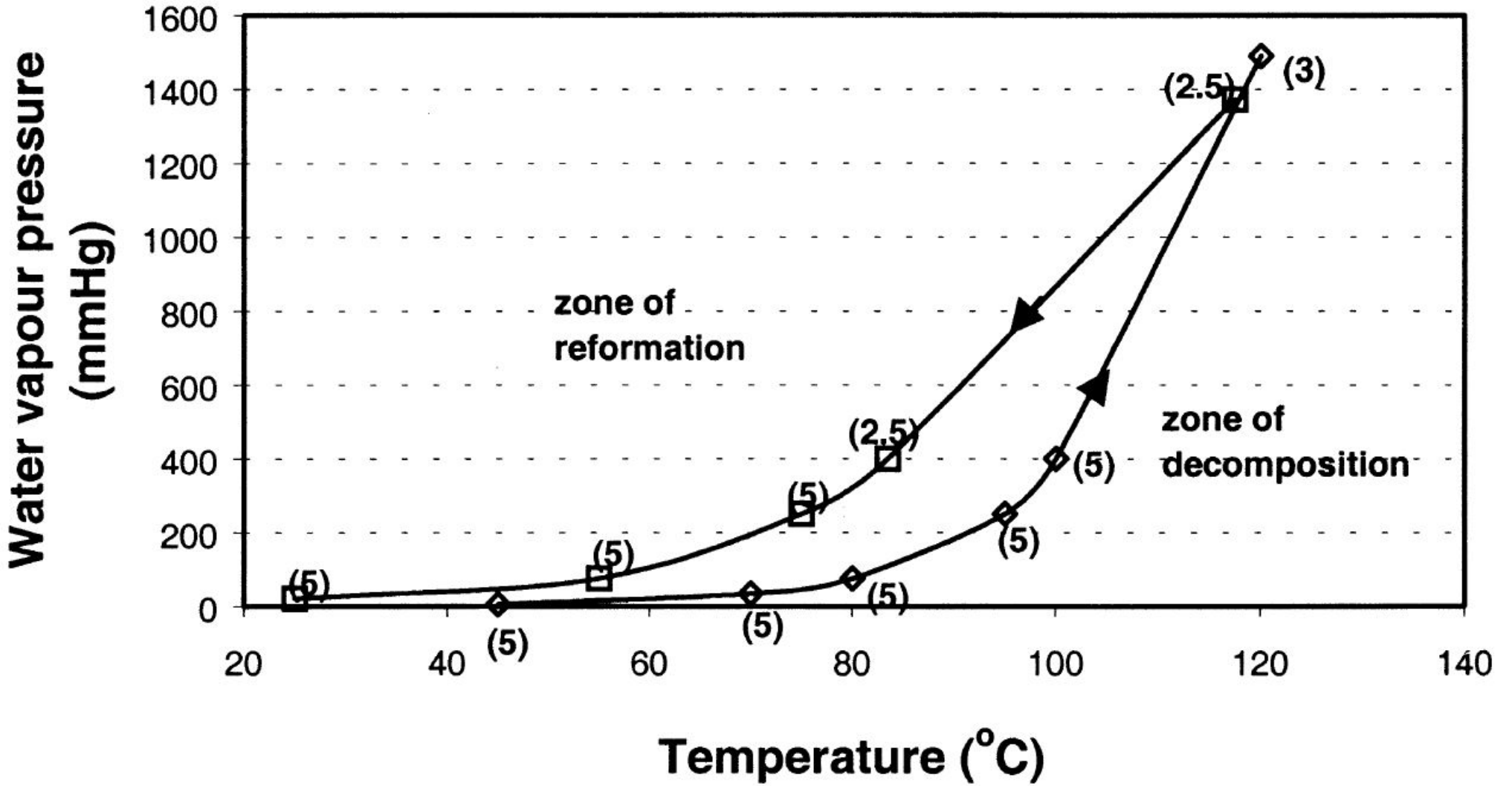
Water vapour pressure (mmHg)
1600
1400
1200
1000
800
600
400
200
0
20
40
60
80
100
120
140
Temperature (°C)
zone of reformation
zone of decomposition
(5)
(5)
(5)
(2.5)
(5)
(5)
(5)
(5)
(2.5)
(3)

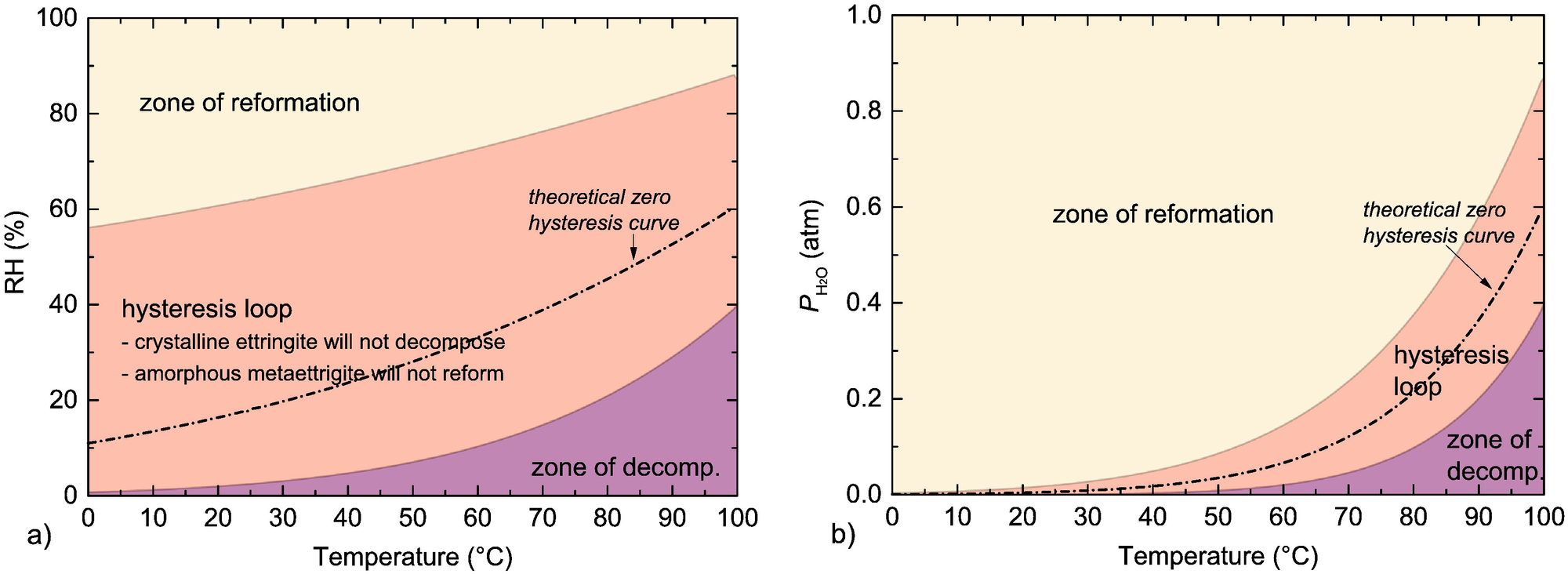
a)
RH (%)
Temperature (°C)
zone of reformation
theoretical zero
hysteresis curve
hysteresis loop
- crystalline ettringite will not decompose
- amorphous metaettrigite will not reform
zone of decomp.
b)
P_{H_2O} (atm)
Temperature (°C)
zone of reformation
theoretical zero
hysteresis curve
hysteresis
loop
zone of
decomp.

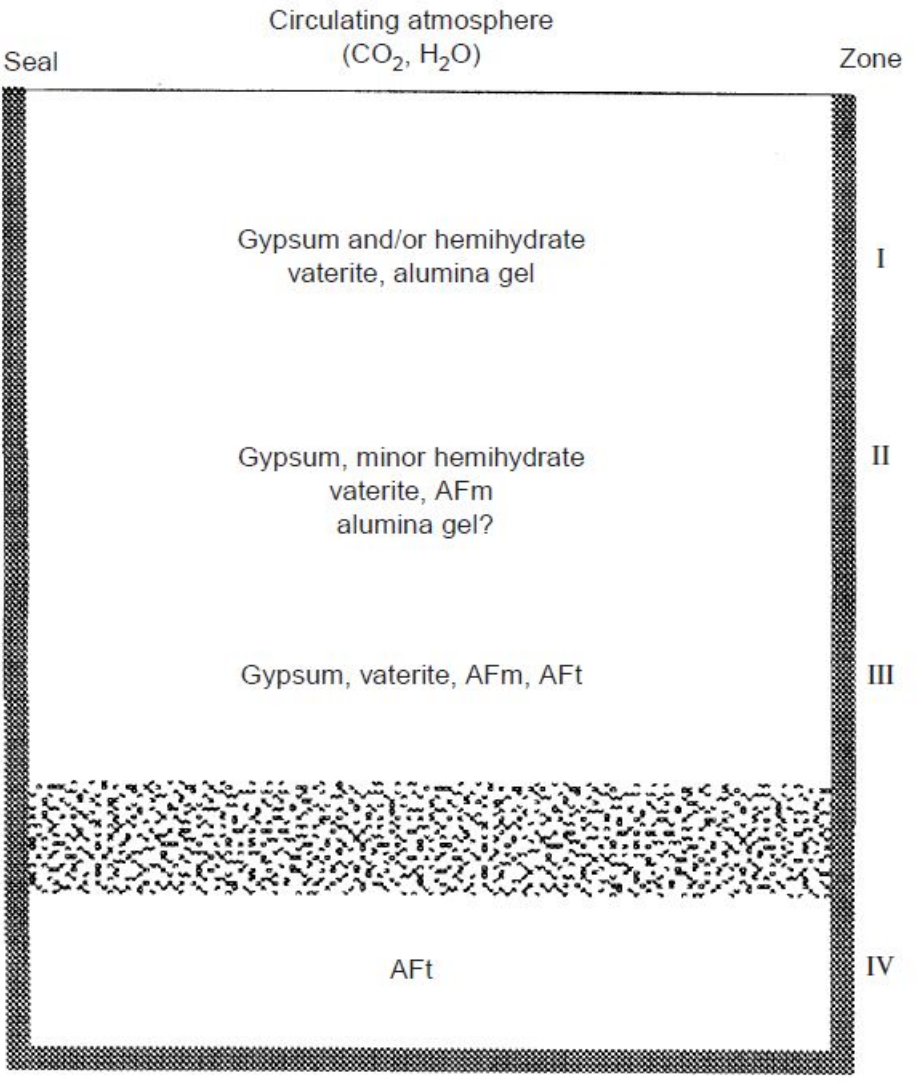
Circulating atmosphere
(CO_2, H_2O)
Seal
Zone
Gypsum and/or hemihydrate
vaterite, alumina gel
I
Gypsum, minor hemihydrate
vaterite, AFm
alumina gel?
II
Gypsum, vaterite, AFm, AFt
III
AFt
IV

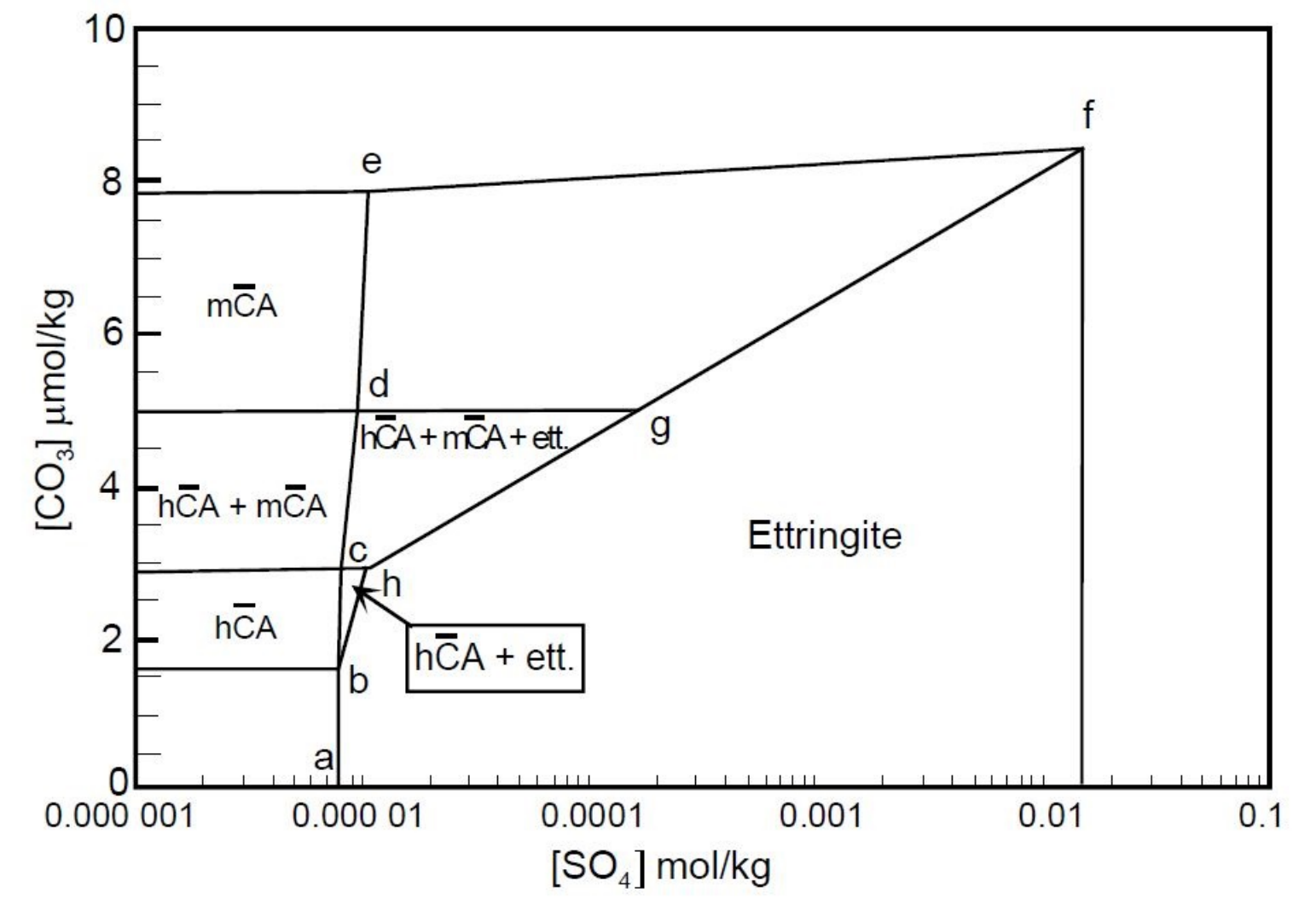
10
8
6
4
2
0
[CO3] µmol/kg
0.000 001
0.000 01
0.0001
0.001
0.01
0.1
[SO4] mol/kg
a
b
c
d
e
f
g
h
mCA
hCA + mCA
hCA
hCA + mCA + ett.
hCA + ett.
Ettringite